JVI Journals.ASM.org

Particle Conformation Regulates Antibody Access to a Conserved GII.4 Norovirus Blockade Epitope

Lisa C. Lindesmith,[a] Eric F. Donaldson,[a] Martina Beltramello,[b] Stefania Pintus,[b] Davide Corti,[b,c] Jesica Swanstrom,[a] Kari Debbink,[a] Taylor A. Jones,[a] Antonio Lanzavecchia,[b,d] Ralph S. Baric[a]

Department of Epidemiology, University of North Carolina, Chapel Hill, North Carolina, USA[a]; Institute for Research in Biomedicine, Bellinzona, Switzerland[b]; Humabs BioMed SA, Bellinzona, Switzerland[c]; Institute of Microbiology, ETH Zurich, Zurich, Switzerland[d]

ABSTRACT

GII.4 noroviruses (NoVs) are the primary cause of epidemic viral acute gastroenteritis. One primary obstacle to successful NoV vaccination is the extensive degree of antigenic diversity among strains. The major capsid protein of GII.4 strains is evolving rapidly, resulting in the emergence of new strains with altered blockade epitopes. In addition to characterizing these evolving blockade epitopes, we have identified monoclonal antibodies (MAbs) that recognize a blockade epitope conserved across time-ordered GII.4 strains. Uniquely, the blockade potencies of MAbs that recognize the conserved GII.4 blockade epitope were temperature sensitive, suggesting that particle conformation may regulate functional access to conserved blockade non-surface-exposed epitopes. To map conformation-regulating motifs, we used bioinformatics tools to predict conserved motifs within the protruding domain of the capsid and designed mutant VLPs to test the impacts of substitutions in these motifs on antibody cross-GII.4 blockade. Charge substitutions at residues 310, 316, 484, and 493 impacted the blockade potential of cross-GII.4 blockade MAbs with minimal impact on the blockade of MAbs targeting other, separately evolving blockade epitopes. Specifically, residue 310 modulated antibody blockade temperature sensitivity in the tested strains. These data suggest access to the conserved GII.4 blockade antibody epitope is regulated by particle conformation, temperature, and amino acid residues positioned outside the antibody binding site. The regulating motif is under limited selective pressure by the host immune response and may provide a robust target for broadly reactive NoV therapeutics and protective vaccines.

IMPORTANCE

In this study, we explored the factors that govern norovirus (NoV) cross-strain antibody blockade. We found that access to the conserved GII.4 blockade epitope is regulated by temperature and distal residues outside the antibody binding site. These data are most consistent with a model of NoV particle conformation plasticity that regulates antibody binding to a distally conserved blockade epitope. Further, antibody "locking" of the particle into an epitope-accessible conformation prevents ligand binding, providing a potential target for broadly effective drugs. These observations open lines of inquiry into the mechanisms of human NoV entry and uncoating, fundamental biological questions that are currently unanswerable for these noncultivatable pathogens.

Noroviruses (NoVs) are the primary cause of severe acute viral gastroenteritis (1). In the United States alone, the annual NoV disease burden is estimated to be $2 billion and 5,000 quality-adjusted life years (2). Globally, NoV-associated deaths are estimated at 200,000 per year (3). Usually, disease severity is modest, but our awareness of morbidity and mortality rates, particularly among the young, elderly, and immunocompromised, is increasing (4–14). An effective vaccine would benefit not only these highly susceptible populations, but also military, child care, health care, and food industry personnel. The primary obstacles to development of an effective NoV vaccine are the large number of antigenic variants, viral evolution, and an incomplete understanding of the components of protective immunity. A monovalent NoV vaccine based on Norwalk virus virus-like particles (VLPs) has been demonstrated to be safe and effective at mitigating the risk of NoV illness and infection (15, 16). Although this is an important first step, additional studies that include NoV strains of more epidemiological relevance are needed to address the fundamental immunogenetic questions surrounding NoV susceptibility and protection from infection.

Strains from the GII.4 genotype cause 70 to 80% of norovirus outbreaks, including four pandemics in the last 15 years. Strain US95/96 (GII.4.1997) caused the pandemic during the mid-1990s (17, 18), followed by the Farmington Hills strain (GII.4.2002) (19), the Hunter strain (GII.4.2004) (20–22), and the Minerva 2006b strain (GII.4.2006) (10, 21, 23). Although the number of documented outbreaks did not significantly increase, GII.4.2006b was subsequently replaced by the global circulating strain New Orleans (GII.4.2009) (1, 24). In 2012, the newly emerged Sydney strain (GII.4.2012) (25, 26) became the predominant circulating NoV strain worldwide. This pattern of emergent strain replacement of a circulating strain followed by periods of stasis is indicative of epochal evolution and results in new GII.4 strains with altered antigenicity and ligand binding profiles (27, 28). Impor-

Received 25 April 2014 Accepted 20 May 2014
Published ahead of print 28 May 2014
Editor: T. S. Dermody
Address correspondence to Ralph S. Baric, rbaric@email.unc.edu.

doi:10.1128/JVI.01192-14

tantly, of the NoVs studied, epochal evolution appears to be restricted to GII.4 NoV strains over the past 25 years.

Currently, there is no validated cell culture model for human norovirus cultivation. As members of the family *Caliciviridae*, NoVs contain positive-sense, single-stranded RNA genomes of about 7.5 kb. Currently, there are five identified genogroups. Almost all human NoV infections are caused by strains from genogroup I (GI) and GII. Each of these genogroups is further subdivided into 9 and 21 different genotypes, respectively, based primarily on the amino acid sequence of the major capsid protein encoded by open reading frame 2 (ORF2) (29). When ORF2 is expressed *in vitro*, an abundance of the major capsid protein is produced (30). Monomers of the major capsid protein first form dimers; then, 90 dimers self-assemble into icosahedral VLPs that are morphologically and antigenically indistinguishable from native virions (31). The capsid protein itself is divided into three structural domains. The shell (S) domain forms the core of the particle, and the protruding (P) domain is divided into two subdomains: protruding subdomain 1 (P1; residues 226 to 278 and 406 to 530) forms a stalk that extends away from the central core supporting P2 (residues 279 to 405) (31). The P2 subdomain is the most surface-exposed region of the particle and has been shown to interact with potential neutralizing/blockade antibodies and carbohydrate binding ligands, such as synthetic histo-blood group antigens (HBGAs), human saliva, and pig gastric mucin (PGM) (28, 32–36). In the GII.4 strains, residues of the P2 subdomain are under selective pressure by the host immune response; this pressure drives viral evolution, resulting in antigenic drift and escape from herd immunity (28, 35, 37). The lack of a cell culture system for NoV propagation prompted us to develop an *in vitro* surrogate neutralization assay, or antibody "blockade" assay, that measures the capacity of an antibody to block binding of a VLP to a carbohydrate ligand (28, 35, 38, 39). Importantly, the blockade assay has been verified by other groups as a surrogate neutralization assay in infected chimpanzees (40) and Norwalk virus-challenged people (15, 41). The surrogate neutralization blockade assay has been critical in mapping evolving GII.4 blockade antibody epitopes in strains antigenically too similar to be differentiated by enzyme immunoassay (EIA) (28, 42).

In addition to antigenic drift, several other viral factors correlate with new GII.4 strain emergence, including strain recombination (43) and polymerase fidelity (44, 45). Unfortunately, the absence of a standard infection model other than humans limits the possibility to study these mechanisms of viral immune evasion in depth. To date, only antigenic drift has been shown to directly impact the effectiveness of the human immune response to mitigate NoV infection. Using anti-GII.4 NoV human monoclonal antibodies (MAbs), we have mapped evolving GII.4 blockade epitopes (46, 47). Changes in these epitopes correlate not only with the emergence of new strains, but also with loss of antibody blockade activity, providing direct evidence that new GII.4 strains are serial human herd immunity escape variants. Many groups have used bioinformatics tools to predict potential GII.4 antibody epitopes (20, 27, 28, 48, 49). By coupling a large panel of anti-NoV MAbs with molecular genetic approaches, we have validated three evolving GII.4 blockade epitopes. Epitope A (residues 294, 296 to 298, 368, and 372) is highly variable and changes with each new GII.4 strain emergence (35, 36, 46, 47). Epitope D (residues 393 to 395) is an evolving blockade epitope that also modulates HBGA binding of GII.4 strains, providing mechanistic support for the observed correlation between epitope escape from herd immunity and altered HBGA binding (28, 47, 49). Epitope E (residues 407, 412, and 413) is a confirmed GII.4.2002 Farmington Hills-specific blockade epitope (36).

We have also described a GII.4-conserved, conformation-dependent blockade epitope recognized by human MAb NVB 71.4 (47). Although this epitope is conserved across GII.4 strains that circulated between 1987 and 2012, NVB 71.4 does not have equivalent blockade capacities for all GII.4 VLPs, suggesting the antibody binds to a complex epitope comprised of both conserved and variable residues. NVB 71.4 has diagnostic and therapeutic potential, and mapping of the epitope recognized by human MAb NVB 71.4 may provide a target for widely protective NoV drugs or vaccine design.

In this study, we demonstrate that the antibody NVB 71.4 cross-blockade and access to the conserved GII.4 blockade epitope are regulated by particle conformation, temperature, and amino acid residues positioned outside the antibody binding site. Strategies to control particle conformation changes will inform NoV immunogen presentation in VLP-based vaccines and therapeutics.

MATERIALS AND METHODS

Virus-like particles. Synthetically derived (Bio Basic Inc., Amherst, NY) epitope-engineered or outbreak strain ORF2 genes were inserted directly into the Venezuelan equine encephalomyelitis (VEE) replicon vector for the production of virus replicon particles (VRPs), as described previously (35, 42). Bac-GII.4.2009 (New Orleans) VLPs were the kind gift of Jan Vinje, Centers for Disease Control and Prevention, Atlanta, GA, and were produced by expression in the baculovirus system and purified with a cesium chloride gradient. Uranyl acetate-stained VLPs were visualized by transmission electron microscopy (TEM). Of note, sequences used to produce VLPs were identified from stool samples from multiple infected individuals. Although irregular particles are occasionally seen in all VLP preparations regardless of the vector expression platform (28, 50), ORF2 proteins that self-assemble into plentiful ~40-nm spherical particles that retain robust binding to conformation-dependent monoclonal antibodies and carbohydrate ligands were considered validated for further studies.

Monoclonal antibodies. The characteristics of the antibodies used in this study have been previously published, except those of GII.4.2002.G5. Details are provided in reference 47 for the human MAbs and in references 35 and 51 for the mouse epitope A MAbs. NVB 71.4 is a broad GII.4 blockade human MAb isolated from a healthy blood donor. GII.4.2002.G5 is a mouse MAb generated by hyperimmunization with GII.4.2002 VLPs, as described previously (36). This antibody is now commercially available from Maine Biotech (MAB227P). Fabs were obtained by papain cleavage using papain immobilized on beaded agarose resin (30 IU/mg; Pierce), followed by HiTrap protein A (GE Healthcare) and size exclusion chromatography (Superdex 200; GE Healthcare).

BOB assay. For experiments using human polyclonal serum, human MAbs were purified on protein A or G columns (GE Healthcare) and biotinylated using the EZ-link NHS-PEO solid-phase biotinylation kit (Pierce). The competition between polyclonal serum antibodies and biotinylated human MAbs for binding to immobilized VLPs (1 μg/ml) was measured by EIA. Briefly, plasma samples were added to GII.4.1997- or GII.4.2006-coated plates at different dilutions. After 1 h, biotinylated human MAb was added at a concentration corresponding to 80% of the maximal optical-density (OD) level, and the mixture was incubated at room temperature (RT) for 1 h. The plates were then washed with phosphate-buffered saline (PBS)-0.05% Tween 20, and bound biotinylated human MAb was detected using alkaline phosphatase (AP)-labeled streptavidin (Jackson ImmunoResearch). The percentage of inhibition

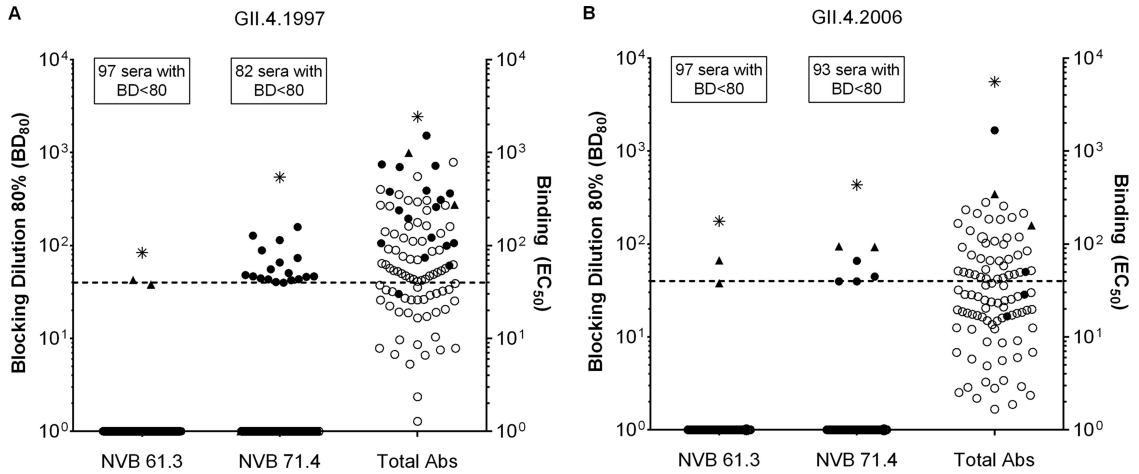

FIG 1 Antibodies to conserved NoV epitopes are rare in human plasma. The ability of human serum samples ($n = 100$) to block binding of human MAbs was evaluated using a BOB assay. Shown are the BD_{80} values of a conserved GII nonblockade epitope antibody (NVB 61.3) and a conserved GII.4 blockade epitope antibody (NVB 71.4) to GII.4.1997 (A) and GII.4.2006 (B) VLPs. Each symbol represents a different individual. BD_{80} values of <40 were scored as negative. Total serum IgG binding to GII.4.1997 and GII.4.2006 was determined by EIA. Reciprocal EC_{50}s are shown on the right. ▲, sera competing for binding of NVB 61.3; ●, sera competing for binding of NVB 71.4; *, donor sources of NVB 61.3 and NVB 71.4.

was tested in duplicate and calculated as follows: {1 − [(OD sample − OD negative control)/(OD positive control − OD negative control)]} × 100. The reciprocal plasma dilution that blocks 80% of binding (BD_{80}) was calculated by interpolation of curves fitted with a 4-parameter nonlinear regression. For screening donor plasma samples and human MAb blocking of binding of mouse MAbs, the binding titers to respective coated VLPs were determined by EIA by measuring the dilution required to achieve 50% maximal binding (50% effective concentration [EC_{50}]), as previously described (47). EIA plates were coated at 0.25 μg/ml VLPs for human MAb blocking of binding (BOB) of mouse MAb assays.

Predicting epitopes. Guided by the empirical data observed for NVB 71.4, which indicated a conserved GII.4 epitope was present, we reasoned that differential binding noted between GII and GII.4 strains could be used to refine the search for a conserved region of the GII.4 capsid sequence. Representative capsid amino acid sequences of GII strains and GII.4 strains (28) from 1974 to 2012 were aligned using ClustalX version 2 (52), and the amino acid residues that were conserved among all GII capsid sequences and all GII.4 capsid sequences were mapped onto the GII.4.2004 (Protein Data Bank [PDB] accession no. 3SJP) (53) crystal structure to identify areas that were conserved among all GII and all GII.4 capsid proteins. The original analysis was performed using the crystal structure for GII.4.1997, as the distances in the structure used for making the epitope prediction are more reliable than those in a homology model. The ERK and EHNQ motifs were identified as regions that were conserved among GII noroviruses and highly conserved among GII.4 viruses. E316, R484, and K493 (ERK) and E488, H501, N522, and Q523 (EHNQ) were identified as conserved residues in these regions that carried a charge and had exposed side chains that protruded. These sites were targeted for mutagenesis using the rationale that preserving the charges of the residues would preserve the structural components necessary for VLP formation. Of note, epitope location predictions were based on VLP structures, not native virion structures.

VLP-carbohydrate ligand binding assay. EIA plates were coated with 10 μg/ml PGM for 4 h and blocked overnight at 4°C in 5% dry milk in PBS-0.05% Tween 20 before the addition of increasing concentrations of VLPs. Bound VLPs were detected with a rabbit anti-GII.4 norovirus polyclonal serum made by hyperimmunization with a cocktail of GII.4.1987, GII.4.2002, GII.4.2006, and GII.4.2009 VLPs, followed by anti-rabbit IgG-horseradish peroxidase (HRP) (GE Healthcare), and the color was developed with 1-Step Ultra TMB ELISA HRP substrate solution (ThermoFisher). Each step was followed by washing with PBS-0.05% Tween 20, and all reagents were diluted in 5% dry milk in PBS-0.05% Tween 20, pH 6.9. VLP binding to PGM is stable between pH 6.3 and 8.1, in agreement with previously published results (54). All incubations were done at room temperature. PGM at 10 μg/ml is a saturating concentration and cannot distinguish carbohydrate affinities between VLPs, but it does give the maximum binding potential of the entire panel of GII.4 VLPs. Half-maximal binding (EC_{50}) values were calculated using sigmoidal dose-response analysis of nonlinear data in GraphPad Prism 6. The percentage of maximum binding was compared to the mean optical density at 450 nm (OD_{450}) of 12 μg/ml VLPs.

VLP-carbohydrate ligand binding antibody blockade assay. For blockade assays, PGM-coated plates were prepared as described above. VLPs (0.25 μg/ml) were pretreated with decreasing concentrations of test MAb for 1 h before being added to the carbohydrate ligand-coated plates for 1 h. Wash steps and detection of bound VLPs were as described above. The percent control binding was defined as the binding level in the presence of antibody pretreatment compared to the binding level in the absence of antibody pretreatment multiplied by 100. Antibody-VLP and VLP-PGM incubations were done at room temperature or 37°C as indicated. All other incubations were done at room temperature. The blockade data were fitted using sigmoidal dose-response analysis of nonlinear data in GraphPad Prism 6. EC_{50}s were calculated for antibodies that demonstrated blockade of at least 50% at the dilution series tested. Monoclonal antibodies that did not block 50% of binding at the highest dilution tested were assigned an EC_{50} of 2 times the assay upper limit of detection for statistical comparison. EC_{50}s between VLPs were compared using one-way analysis of variance (ANOVA) with the Dunnett posttest when at least three values were compared or Student's *t* test when only two values were compared. A difference was considered significant if the *P* value was <0.05. Of note, VLP concentrations in blockade assays are in the low nanomolar range and therefore cannot discriminate between antibodies with subnanomolar affinities. Antibody-VLP interactions were validated for compliance with the law of mass action by performing blockade assays of GII.4.1997 and GII.4.2006 at 0.25, 0.5, 1, and 2 μg/ml VLPs. EC_{50}s for antibody blockade varied less than 2-fold (1 dilution) between any combination of VLP concentrations tested, indicating that under the test conditions, antibody is in excess of the VLPs and the tenets of the law of mass action are met for antibody-VLP binding (data not shown). Blockade assays using human type A or B saliva as the source of carbohydrate ligand were performed as described previously (55) with 0.5 μg/ml VLPs at room temperature or 37°C.

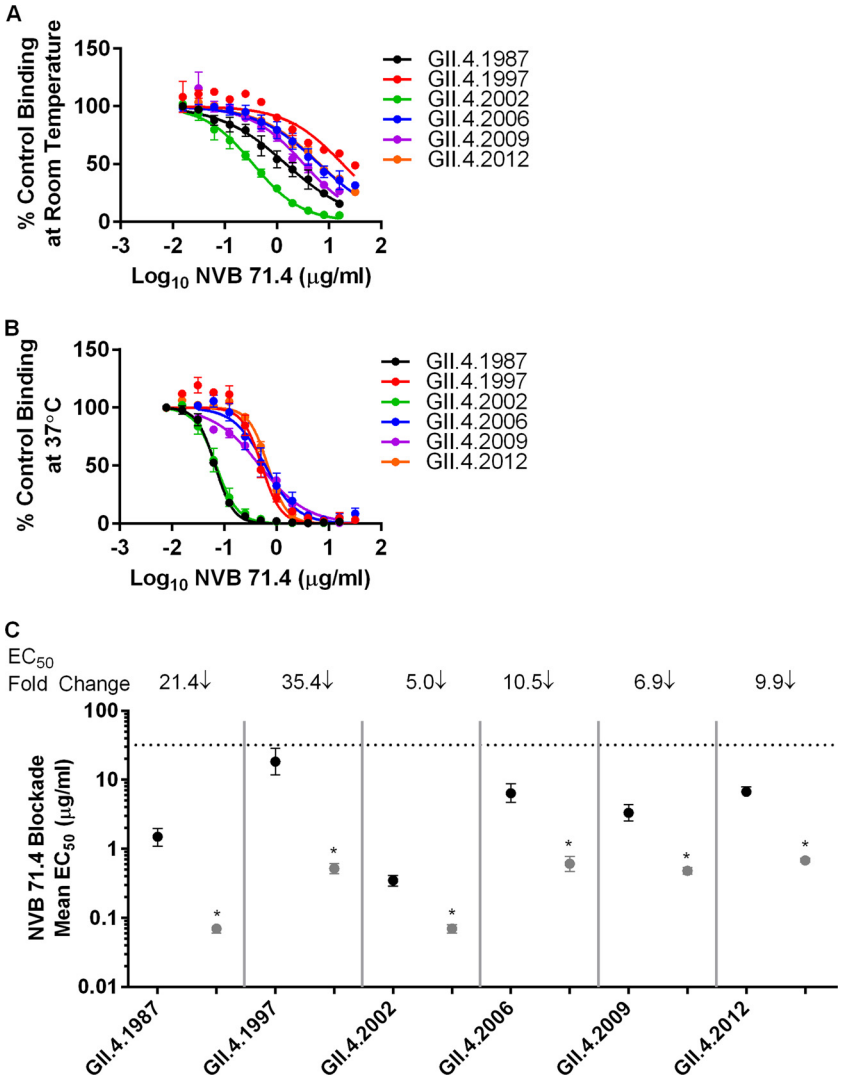

FIG 2 Access of NVB 71.4 to the conserved GII.4 blockade epitope is temperature dependent. NVB 71.4 was assayed for the ability to block the interaction of a panel of time-ordered GII.4 VLPs with carbohydrate ligand. Sigmoidal curves were fitted to the mean percent control binding (the percentage of VLPs bound to ligand in the presence of antibody pretreatment compared to the number of VLPs bound in the absence of antibody pretreatment) at room temperature (A) and at 37°C (B), and the mean EC_{50} titers for blockade at room temperature (solid circles) and at 37°C (grey circles) were calculated and compared (C). The fold change (arrow denotes decrease) in the EC_{50} titer was defined as the mean EC_{50} at 37°C compared to that at room temperature. *, mean EC_{50} blockade titer significantly different between room temperature and 37°C. The dotted line in panel C marks the assay upper limit of detection. The error bars represent the standard errors of the mean (SEM) on the sigmoidal fit curves (A and B) and 95% confidence intervals on the mean EC_{50} graph (C).

Antibody relative affinity measurements. Antibody K_d measurements were done as previously described (56) at room temperature and at 37°C. Serial dilutions were tested in duplicate in at least two independent experiments for each temperature. Briefly, EIA plates were coated with 0.25 μg/ml VLPs in PBS, blocked, and incubated with serial dilutions of test antibody. Bound antibody was detected by anti-human IgG-HRP, and color was developed as described above. K_d values were calculated using the one-site specific-binding equation in GraphPad Prism 6. The K_d values were validated by repeating the above-described assay at a range of VLP concentrations.

VLP protein A-gold staining. VLPs were incubated with 5 μg/ml human MAb at 37°C, followed by 1/100 dilution of protein A conjugated to 10-nm gold particles at room temperature; adsorbed onto prepared grids; stained with 2% uranyl acetate; and visualized by TEM. Staining specificity was validated by counting 50 fields of the negative-control (VLP minus human IgG plus protein A-gold). Only one gold particle was observed near a VLP in the 50 negative-control fields.

RESULTS

Antibodies to conserved NoV epitopes are rarely detected in human serum samples. To estimate the fraction of antibodies specific for conserved GII.4 epitopes in the overall serum antibody response, 100 serum samples collected from healthy individuals were assayed for the ability to block binding of human MAbs NVB 61.3 and NVB 71.4 in a BOB assay (57, 58). Both human MAbs recognize a broad panel of antigenically diverse, epidemiologically significant GII.4 NoV strain VLPs by EIA, but only NVB 71.4 blocks VLP-ligand interactions (47). When tested against GII.4.1997 (Fig. 1A) or GII.4 2006 (Fig. 1B), three sera were able to compete with NVB 61.3 binding while the remaining sera did not show significant inhibition, in spite of variable binding to tested VLPs (Fig. 1A and B, right columns). Eighteen serum samples competed with NVB 71.4 binding to GII.4.1997, and six sera could

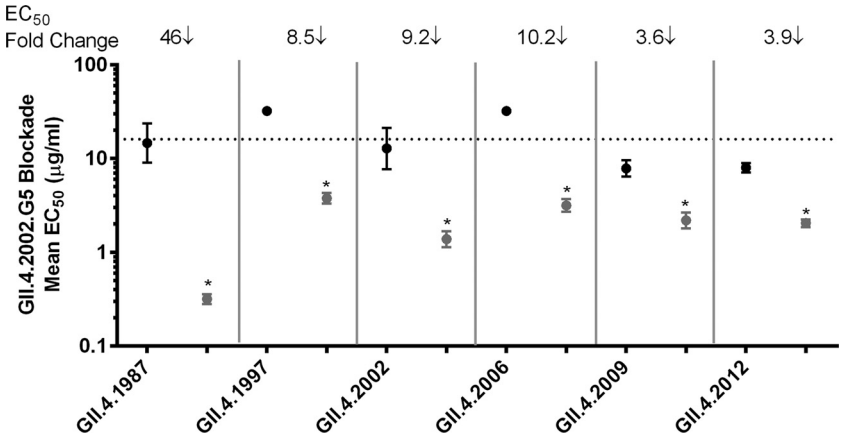

FIG 3 Access of GII.4.2002.G5 to a conserved GII.4 blockade epitope is regulated by temperature. GII.4.2002.G5 was assayed for the ability to block the interaction of GII.4 VLPs with carbohydrate ligand at room temperature (solid circles) and at 37°C (grey circles). Sigmoidal curves were fitted to the mean percent control binding (the percentage of VLPs bound to ligand in the presence of antibody pretreatment compared to the number of VLPs bound in the absence of antibody pretreatment), and the mean EC_{50} titer for blockade was calculated. The fold change (arrow denotes decrease) in the EC_{50} titer was defined as the mean EC_{50} at 37°C compared to that at room temperature. *, mean EC_{50} blockade titer significantly different between room temperature and 37°C. Nonblockade VLPs were assigned an EC_{50} of 2 times the upper limit of detection for statistical analysis and denoted by a data marker on the graph above the dotted line (the assay upper limit of detection) for visual comparison. The error bars represent 95% confidence intervals.

compete for binding to GII.4.2006 (Fig. 1). These data indicate that antibodies to GII.4 conserved epitopes may be rare in human serum samples even if the binding titers to the tested VLPs are high for the majority of the sera (EC_{50}s are reported in Fig. 1A and B, right).

The conserved GII.4 blockade epitope is likely not surface exposed, and antibody access to the epitope is regulated by particle conformation. To characterize the epitope recognized by NVB 71.4, we compared the profiles for NVB 71.4 blockade of a time-ordered panel of GII.4 VLPs representing circulating GII.4 strains from 1987 through 2012. As shown previously (47), blockade curves had relatively shallow slopes (range, 0.68 to 0.92) (Fig. 2A). These data suggest that access of NVB 71.4 to the conserved blockade epitope may be restricted under the test conditions. Therefore, we repeated the blockade assay for NVB 71.4 against the panel of GII.4 VLPs at 37°C to increase the probability of the VLPs adopting a conformation more favorable for antibody binding during the incubation time (59). Incubation at 37°C significantly increased the blockade capacity of NVB 71.4 for the panel of GII.4 VLPs (Fig. 2B). Further, the blockade curves demonstrated steep slopes (range, 1.1 to 2.8), with complete blockade reached at antibody saturation for each VLP. In agreement with previous findings (47), NVB 71.4 did not block each GII.4 VLP equivalently at room temperature and 37°C. Incubation at the higher temperature resulted in significantly less antibody needed for blockade of GII.4.1987 (21.4-fold less), GII.4.1997 (35.4-fold less), GII.4.2002 (5.0-fold less), GII.4.2006 (10.5-fold less), GII.4.2009 (6.9-fold less), and GII.4.2012 (9.9-fold less) (Fig. 2C). Incubation at 37°C did not increase the number of strains blocked by NVB 71.4, as the higher temperature did not allow blockade of any non-GII.4 VLPs tested (data not shown), in agreement with previous findings at room temperature (47). Temperature-dependent NVB 71.4 blockade activity was confirmed with the alternative ligand sources human type A and type B saliva (data not shown). As demonstrated for PGM, all of the tested VLPs were blocked at lower concentrations of NVB 71.4 at 37°C compared to RT. Although the temperature effect was retained across ligand sources, the degree of temperature effect varied both by GII.4 VLP and between the three types of ligand, in agreement with previous reports (28, 47).

In contrast, EC_{50} titers for blockade of surface epitopes A and D were only minimally impacted by temperature. GII.4.2006 blockade by human MAbs that bind to surface-exposed epitopes A and D required 1.4- and 1.3-fold less antibody, respectively, for 50% blockade of binding at 37°C than at room temperature (data not shown). Although the mean EC_{50} titers for blockade of epitopes A and D are significantly different between room temperature and 37°C, the difference between the values reflects less than one 2-fold serial dilution. These data indicate that, unlike epitopes A and D, the conserved blockade epitope recognized by NVB 71.4 may not be readily accessible on the viral particle at all times, resulting in regulated antibody access under the tested conditions.

In our screen of over 100 mouse MAbs against GII.4 VLPs, we identified only one MAb with broad GII.4 blockade activity, and this cross-blockade was temperature dependent (Fig. 3). In agreement with the findings for NVB 71.4, GII.4.2002.G5 mouse MAb did not block each GII.4 VLP equivalently at room temperature and at 37°C. Incubation at the higher temperature resulted in less antibody being needed for blockade of GII.4.1987 (46-fold less), GII.4.1997 (8.5-fold less), GII.4.2002 (9.2-fold less), GII.4.2006 (10.2-fold less), GII.4.2009 (3.6-fold less), and GII.4.2012 (3.9-fold less). Incubation at 37°C did not increase the number of strains blocked (data not shown). The varied degrees of blockade between different GII.4 VLPs suggest that the epitope GII.4.2002.G5 recognizes is composed of both residues that are conserved and residues that are variable across the GII.4 panel, as observed for NVB 71.4 (Fig. 2).

Viruses and virus-like particles are dynamic structures, and the degree of structural flexibility is temperature sensitive and can be influenced by host factors (59–61). While this study is the first to show that VLPs produced from VEE replicons likely adopt different conformations, to our knowledge, no studies have demonstrated that viruses or VLPs assembled in the baculovirus insect cell system, which functions at 27 to 28°C, are similarly dynamic.

Therefore, we compared GII.4.2009 VLPs produced in the baculovirus-based insect system (27°C) and the VEE-based mammalian system (37°C) for antibody blockade at room temperature and at 37°C. Importantly, the primary nucleotide sequences of the two GII.4.2009 capsid constructs are identical (GenBank accession no. ADD10375). For both mammalian and insect cell-produced GII.4.2009 VLPs, blockade of surface epitope A was efficient and not temperature sensitive (≤1.3-fold less antibody was needed for 50% blockade) (Fig. 4A). Unexpectedly, NVB 71.4 blockade was also not temperature sensitive (1.3-fold more antibody was needed at 37°C) for the insect cell-produced VLPs compared to 6.9-fold less antibody needed at 37°C for the mammalian cell-produced VLPs. Further, NVB 71.4 blockade of GII.4.2009 VLPs produced in insect cells required 29.3-fold less antibody for 50% blockade at room temperature and 3.2-fold less at 37°C than GII.4.2009 VLPs produced in mammalian cells (0.1133 and 0.1503 μg/ml compared to 3.322 at room temperature and 0.4817 μg/ml at 37°C) (Fig. 2 and 4B) (47). GII.4.2002.G5 needed 93-fold less antibody at room temperature and 19-fold less at 37°C for 50% blockade for GII.4.2009 VLPs produced in insect cells than for VLPs produced in mammalian cells (0.0843 and 0.1173 μg/ml compared to 7.8 μg/ml at room temperature and 2.177 μg/ml at 37°C) (Fig. 3 and 4C). This lack of temperature effect on Bac-GII.4.2009 blockade was maintained when type B saliva was used as the ligand source and when NVB 71.4 Fab fragments were used for the blocking antibody (data not shown). These data support other study findings suggesting that factors outside the capsid sequence can modify VLP antigenicity in subtle ways and support the hypothesis that antibody access to the conserved GII.4 blockade epitope is regulated by temperature and likely by particle conformation.

Prediction of a conserved GII.4 motif with epitope-like features. Using the crystal structure of the GII.4.2004 P domain dimer (PDB accession no. 3SJP) (53), conserved and variable amino acids were mapped onto the P domain dimer surface. A region that was highly conserved among GII.4 norovirus strains was identified on the side of the P domain dimer (Fig. 5A and B), within the P1 subdomain, interior to the exposed surface of the P2 subdomain, and distal to the carbohydrate binding pockets that correlate with differences in binding to NVB 71.4 (Fig. 5B and C). This region contained several conserved amino acids in an area large enough to represent a potential antibody binding site (>1,000 Å^2), including charged amino acids at positions E316, R484, and K493 (post-1997 GII.4 numbering) (Fig. 5C). These amino acids were named the ERK motif (Fig. 5C). The ERK motif is highly conserved among GII.4 strains that circulated between 1987 and 2012 and was predicted to be either a binding site for or a regulator of NVB 71.4 binding. In addition, amino acid position 310 was identified as a site of variation among contemporary GII.4 epidemic strains (2009 and 2012) that was proximal to the highly conserved region containing the ERK motif (Fig. 5D).

Conservation of the ERK motif and its subsurface P1 location indicated that changes in these residues could be detrimental to viral particle structure or stability. Therefore, to evaluate the impact of the ERK motif on antibody blockade activity, we designed mutant VLPs in the GII.4.2006 backbone that conserved the residue charge but changed the residue side chain length. The GII.4.2006.ERK clone contains substitutions E316D, R484K, and K493R (Fig. 6A). For comparison, we designed an additional P1 domain mutant based on a conserved GII antibody epitope recently published (62). GII.4.2006.EHNQ contains mutated resi-

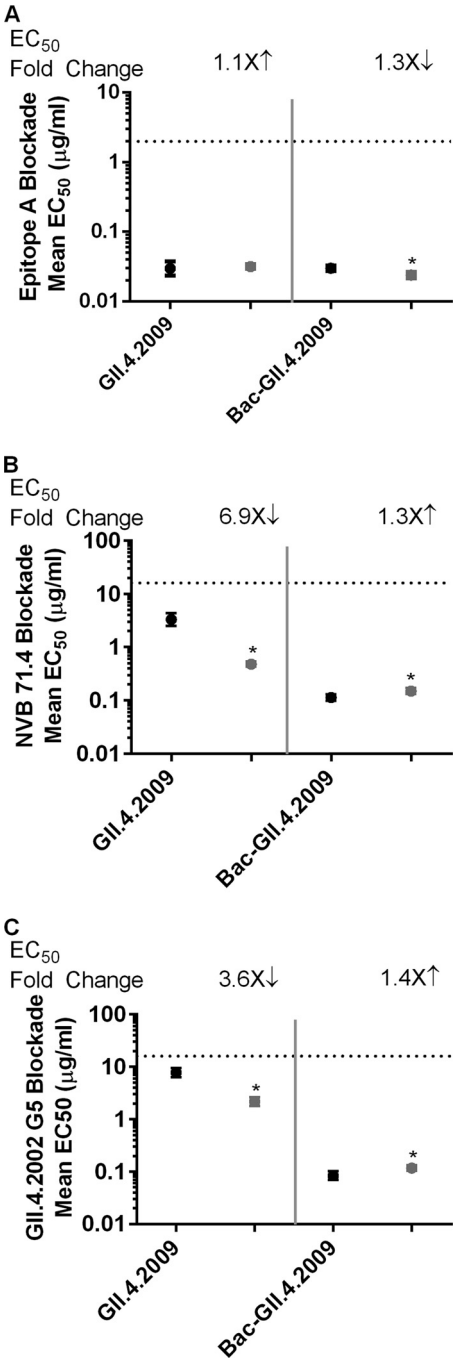

FIG 4 Antibody access to the conserved epitope is not temperature sensitive on GII.4.2009 VLPs made at lower temperature in insect cells. Epitope A human MAb (A), NVB 71.4 (B), and GII.4.2002.G5 (C) were assayed for the ability to block the interaction of GII.4.2009 VLPs produced in insect cells using a baculovirus expression system and carbohydrate ligand at room temperature (solid circles) and at 37°C (grey circles). Sigmoidal curves were fitted to the mean percent control binding (the percentage of VLPs bound to ligand in the presence of antibody pretreatment compared to the number of VLPs bound in the absence of antibody pretreatment), and the mean EC_{50} titer for blockade was calculated. The fold change (arrow denotes increase or decrease) in the EC_{50} titer was defined as the mean EC_{50} at 37°C compared to that at room temperature. *, mean EC_{50} blockade titer significantly different between room temperature and 37°C. The error bars represent 95% confidence intervals.

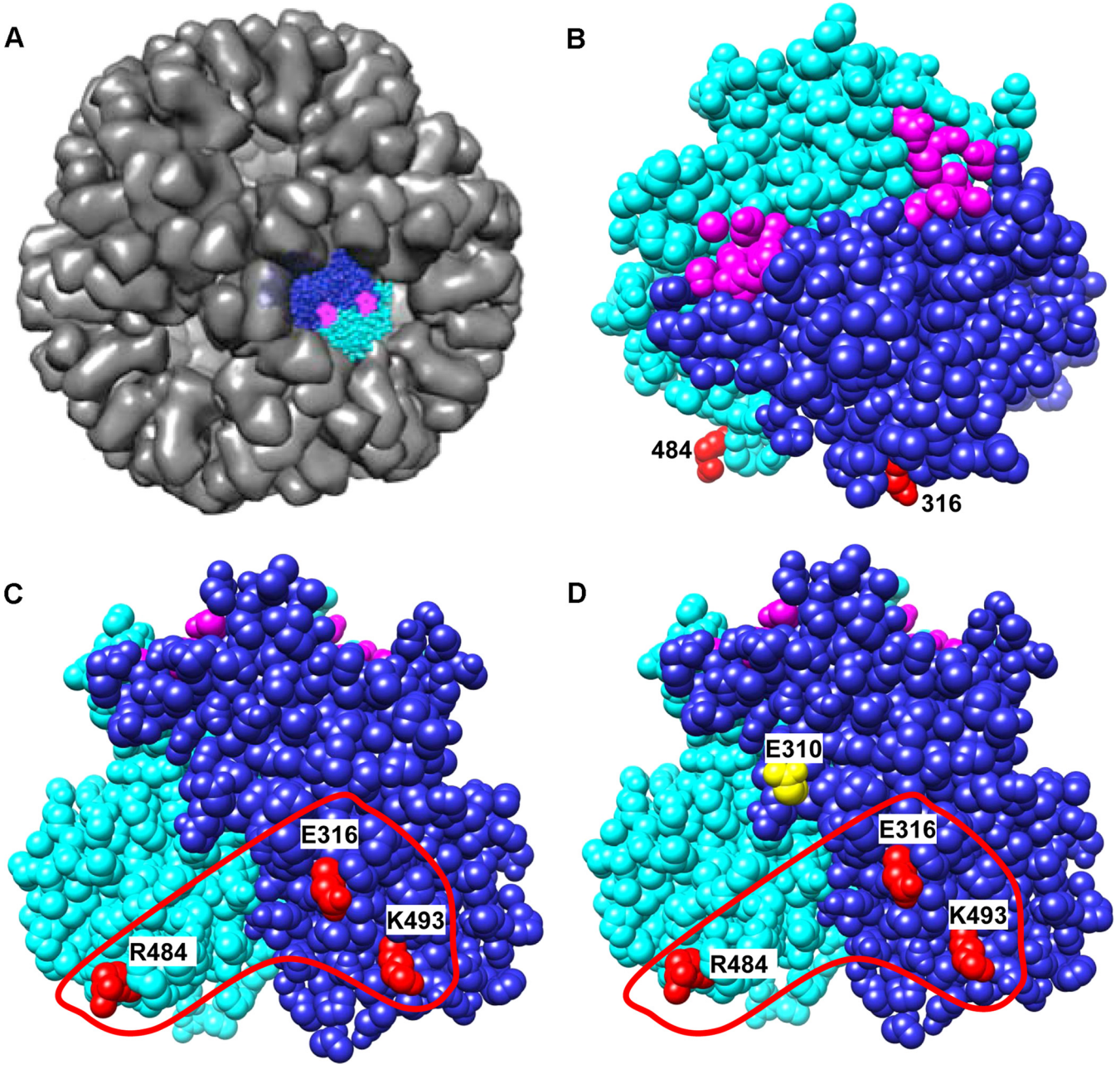

FIG 5 Predicting a conserved epitope. Shown are chain A (dark blue) and chain B (light blue) of the protruding domain structure. (A) The P1 subdomain is highly conserved among GII.4 epidemic strains and is hidden from the surface in the context of the VLP superstructure. The carbohydrate binding pocket (pink) is located in the P2 subdomain, which is exposed on the surface of the VLP. (B) A conserved region was identified on the side of the P domain dimer distal to the binding pockets with sites of variation (red) that correlated with phenotypic differences among GII.4 VLPs. (C) The ERK motif (rotated 60° counterclockwise on the *x* axis compared to panel B) is comprised of three charged amino acids that are found at positions 316, 484, and 493 (red) in the conserved region (circled in red) that is predicted to interact with NVB 71.4. (D) Variation at position 310 (yellow) is proximal to the conserved region and may regulate binding to this conserved site.

dues E488D, H501K, N522Q, and Q523N (post-1997 GII.4 numbering) (Fig. 6A). The GII.4.2006.ERK substitutions did not notably alter the particle structure as measured by electron microscopy (EM) visualization of ~40-nm spherical particles and ligand binding ability similar to that of GII.4.2006. However, microscopic visualization of the GII.4.2006.EHNQ mutant revealed numerous irregular structures but no ~40-nm spherical particles. Corresponding to the lack of particle integrity, this mutant was unable to bind carbohydrate ligand (Fig. 6B and C). Having failed VLP manufacturing quality control, no additional studies were performed with mutant GII.4.2006.EHNQ.

The GII.4 conserved ERK motif impacts NVB 71.4 and GII.4.2002.G5 blockade capacity with little impact on temperature sensitivity. As the substitutions made within GII.4.2006.ERK

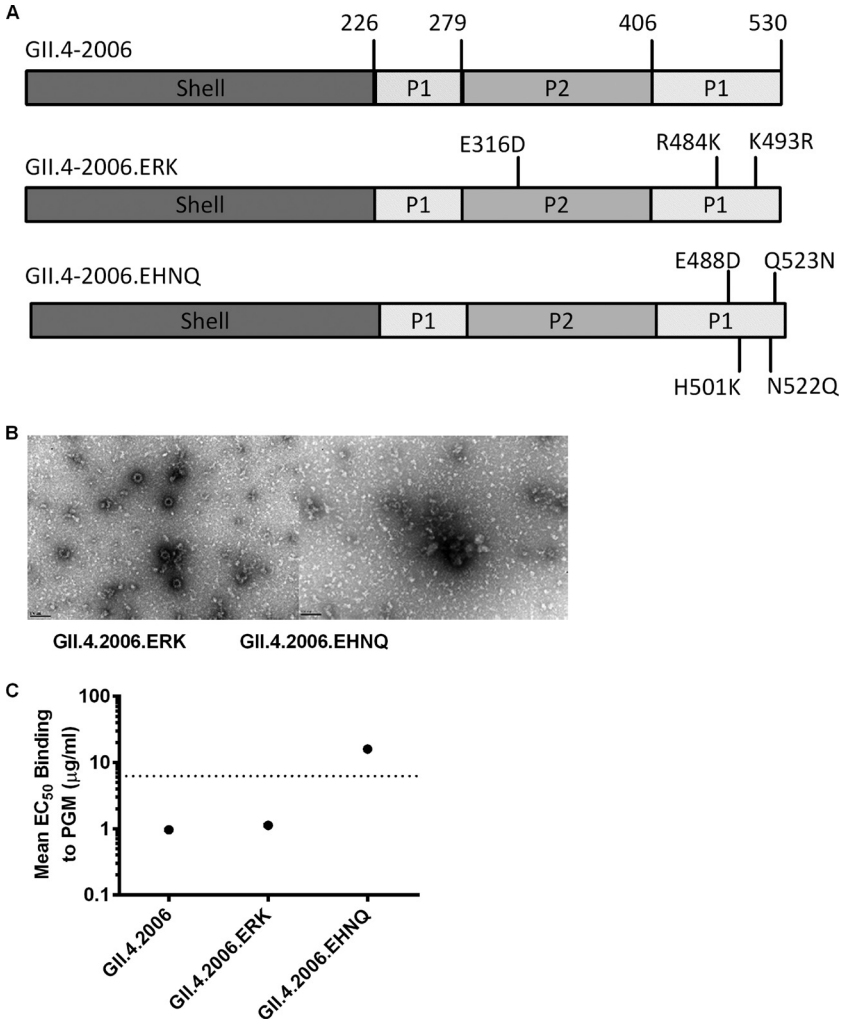

FIG 6 Characterization of VLPs with substitutions in predicted conserved antibody epitopes. (A) Schematic of constructs. (B and C) Particle integrity was verified by transmission electron microscope visualization (B) and carbohydrate ligand (PGM type III) binding of VLPs (C). Non-PGM-binding VLPs were assigned an EC_{50} of 2 times the upper limit of detection for statistical analysis and denoted by a data marker on the graph above the dotted line (the assay upper limit of detection) for visual comparison. The error bars represent 95% confidence intervals. Scale bars, 100 nm.

retained ligand binding activity, we evaluated the impacts of these residue changes on the blockade potencies of NVB 71.4, GII.4.2002.G5, and antibodies to surface-exposed epitopes. ERK substitutions resulted in minimal increases in blockade ability for both epitope A and D antibodies (1.3-fold less antibody was needed for 50% blockade at 37°C than at room temperature for both human MAbs) (data not shown). However, the ERK motif substitutions resulted in complete loss of blockade potency of NVB 71.4 at room temperature. Blockade potency was restored at 37°C (2.519 μg/ml), although significantly more antibody (4.1-fold) was needed for blockade than for GII.4.2006 (Fig. 7A). Similarly, GII.4.2002.G5 did not block GII.4.2006.ERK at room temperature but gained limited blockade potency at 37°C (11.43 μg/ml) (Fig. 7B). However, significantly more antibody (3.6-fold) was needed for blockade of GII.4.2006.ERK than for GII.4.2006 even at the elevated temperature. Further, blockade of GII.4.2006 and GII.4.2006.ERK with NVB 71.4 Fab fragments was more potent (lower EC_{50}) than with NVB 71.4 IgG but similarly temperature sensitive. Notably, the EC_{50}s were 2.1-fold different at room temperature (1.758 versus 0.8052) and 1.4-fold different at 37°C (0.1807 compared to 0.1259), indicating that with the smaller epitope-binding molecule, the ERK residues do not effect antigenicity (Fig. 7C). Further, ERK substitutions negatively impact blockade potency for both conserved epitope antibodies but do not negate the compensatory effect of incubation at higher temperature, indicating that the ERK residues may affect antibody access to the epitope instead of the antibody binding strength for the epitope.

Quantitative EIAs (56) further indicated that ERK residue substitutions do not affect antibody affinities. Based on the differences in blockade titers, if the ERK substitutions primarily affected antibody affinity, we would expect a 10-fold change in functional affinity for NVB 71.4 at room temperature and a 4-fold change at 37°C. However, there is less than a 2-fold difference (one serial dilution) between the antibody functional affinities (K_d values) of NVB 71.4, GII.4.2002.G5, and epitope D human MAb for GII.4.2006 and GII.4.2006.ERK VLPs between room temperature and 37°C (Table 1), clearly indicating that the ERK motif is not the antibody binding site.

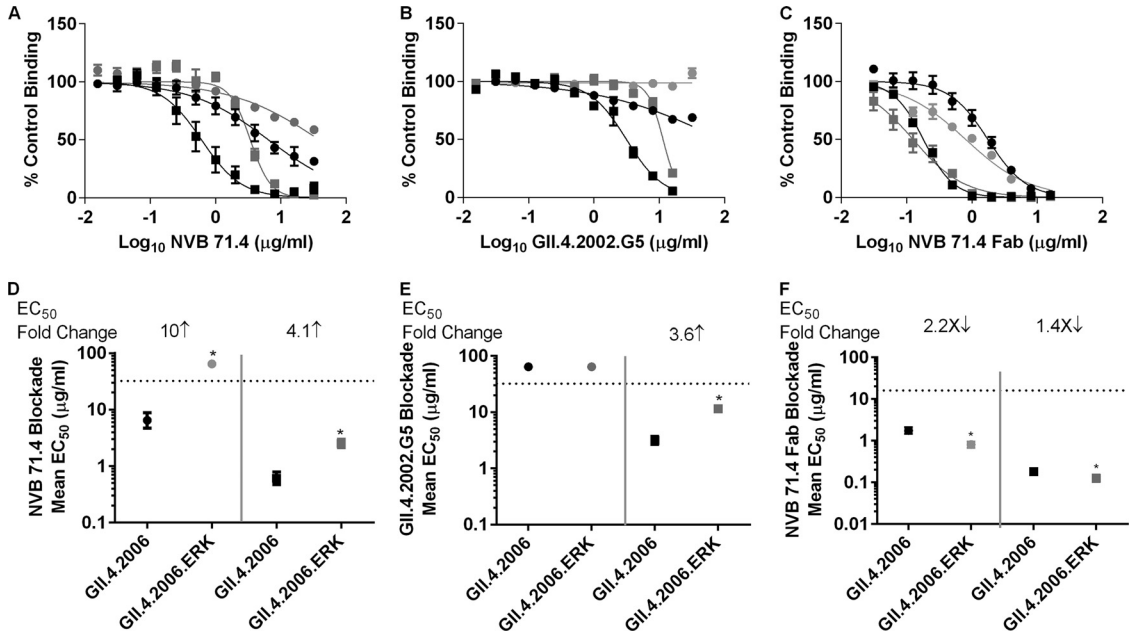

FIG 7 ERK motif substitutions decrease NVB 71.4 and GII.4.2002.G5 blockade potential with little impact on blockade temperature sensitivity. NVB 71.4 (A and D), GII.4.2002.G5 (B and E), and NVB 71.4 Fab (C and F) were assayed for the ability to block carbohydrate ligand interaction of GII.4.2006 VLPs at room temperature (solid circles) and at 37°C (solid squares) and GII.4.2006.ERK VLPs at room temperature (grey circles) and 37°C (grey squares). Sigmoidal curves were fitted to the mean percent control binding (the percentage of VLPs bound to ligand in the presence of antibody pretreatment compared to the number of VLPs bound in the absence of antibody pretreatment), and the mean EC_{50} titers for blockade were calculated and compared. The fold change (arrow denotes increase or decrease) in the EC_{50} titer was defined as the mean EC_{50} at 37°C compared to that at room temperature. *, mean EC_{50} blockade titer for GII.4.2006.ERK significantly different from the mean EC_{50} blockade titer for GII.4.2006 at the same temperature. Nonblockade VLPs were assigned an EC_{50} of 2 times the upper limit of detection for statistical analysis and denoted by a data marker on the graph above the dotted line (the assay upper limit of detection) for visual comparison. The error bars represent the SEM on sigmoidal fit curves (A to C) and 95% confidence intervals on the mean EC_{50} graphs (D to F).

Residue 310 modulates antibody blockade potency and temperature sensitivity. Dominant GII.4 strains circulating between 1987 and 2006 conserved an asparagine at residue 310. With the emergence of GII.4.2009, N310 became S310. Subsequently, GII.4.2012 replaced the serine at 310 with an aspartic acid (Fig. 8B). To investigate the role of residue 310 in GII.4 VLPs, we first developed mutated VLPs that exchanged the 310 residue between GII.4.2009 and GII.4.2012 (Fig. 9A). These substitutions did not notably alter the particle structure as measured by electron microscopy visualization and ligand binding ability (Fig. 9B and C) or blockade by epitope A or D human MAbs (data not shown). In these constructs, the ERK motif was unchanged. For both NVB 71.4 and GII.4.2002.G5, exchange of residue 310 between GII.4.2009 and GII.4.2012 resulted in an exchange of potency and temperature sensitivity phenotypes (Fig. 10A and B and data not shown). GII.4.2009.S310D blockade potency decreased 2- and 4.1-fold and temperature sensitivity increased 10.5- and 12-fold for NVB 71.4 and GII.4.2002.G5, respectively. Conversely, GII.4.2012.D310S blockade potency increased 2.7- and 3.2-fold and temperature sensitivity decreased 4.6- and 3.1-fold for each antibody. NVB 71.4 Fab had modestly increased potency at room temperature (1- to 2.8-fold) for the 310 mutant VLPs, and the blockade was less temperature sensitive (2.4- to 8.0-fold) than the wild type, indicating that the smaller molecule has better access to the epitope.

To evaluate the interplay between residue 310 and the ERK motif, we created VLP GII.4.2009.NERK containing both the S310D and ERK substitutions (S310D, E316D, R484K, and K493R) (Fig. 9A). This VLP is called NERK instead of SERK because of the asparagine found at 310 in the GII.4 VLPs from 1987 to 2006. Interestingly, combining the 310 and ERK residue changes in the GII.4.2009 backbone resulted in a VLP that was blocked similarly to GII.4.2009 for NVB 71.4 but required 4.1-fold more GII.4.2002.G5 for 50% blockade. Of note, for both IgGs and NVB 71.4 Fab, the NERK substitutions reduced the advantage of incubating at higher temperature by ~50% compared to wild-type VLP blockade. As there was less than a 2-fold difference in K_d values for NVB 71.4 or GII.4.2002.G5 binding to GII.4.2009 and GII.4.2009.NERK at room temperature or 37°C (data not shown), it is unlikely that NERK forms the antibody epitope; instead, 310 and the ERK residues together form a regulating network. Blockade by anti-epitope A and D human MAbs was unaffected by the

TABLE 1 Monoclonal antibody functional affinities for GII.4.2006 and GII.4.2006.ERK at room temperature and 37°C

		K_d (nM) ± SEM	
MAb	Temp (°C)	GII.4.2006	GII.4.2006.ERK
NVB 71.4	RT	0.48 ± 0.09	0.56 ± 0.01
	37	0.27 ± 0.01	0.29 ± 0.05
GII.4.2002.G5	RT	1.0 ± 0.24	2.0 ± 0.29
	37	0.57 ± 0.05	0.87 ± 0.11
Epitope D	RT	0.78 ± 0.09	0.95 ± 0.13
	37	0.39 ± 0.07	0.41 ± 0.05

A

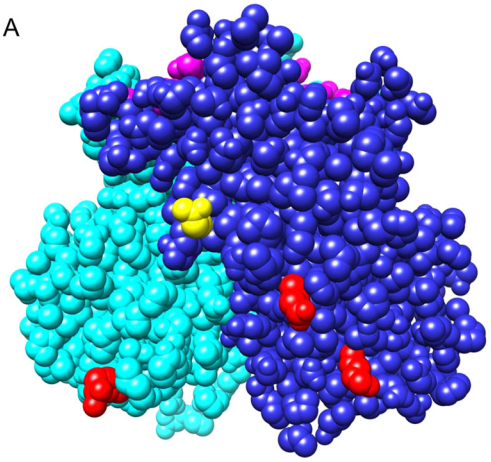

B

	Predicted Motif "NERK"			
VLPs	310	316	484	493
GII.4.1987	N	E	R	K
GII.4.1997	N	E	R	K
GII.4.2002	N	E	R	K
GII.4.2004	N	E	R	K
GII.4.2006	N	E	R	K
GII.4.2009	S	E	R	K
GII.4.2012	D	E	R	K

FIG 8 Predicting residues that interact with the ERK motif. (A) The ERK motif was mapped onto the crystal structure of GII.4.2004 to identify sites that may be interacting with the ERK motif. (B) The ERK motif is highly conserved among epidemiologically important GII.4 strains, while residue 310 has evolved in the most recent GII.4 strains with global distribution.

310 or NERK residue mutation, indicating that the substitutions specifically targeted the conserved blockade epitopes and did not cause global particle disturbances (data not shown). These data indicate that in multiple GII.4 backbones residue 310 has a subtle effect on blockade potency at room temperature and a more significant effect on the temperature sensitivity of the conserved blockade epitope. Comparison of the effects of serine versus aspartic acid at position 310 indicates better access to the epitope because variation in regulating residues reduces the effect of incubation at higher temperature.

NVB 71.4 VLP-ligand interaction blockade is not explained by particle disassembly or steric hindrance. To explore the mechanisms of NVB 71.4 blockade, we stained GII.4.2009 and GII.4.2009.NERK VLPs with NVB 71.4 and epitope A human MAbs and protein A gold particles and observed antibody-labeled VLPs by negative-stain electron microscopy (Fig. 11). Both NVB 71.4 and the epitope A human MAbs labeled intact VLPs, indicating that the antibody-induced lack of ligand binding was not the result of antibody-mediated particle disassembly or that NVB 71.4 preferentially binds to disassembled capsid protein. To evaluate if NVB 71.4 binding to subsurface sites altered the particle surface in a way that was undetectable by EM but rendered the particle not amenable to interactions at the surface, antibody blockade-of-binding competition assays were performed using antibodies to surface-exposed, conformation-dependent epitope A and subsurface, conformation-dependent NVB 71.4 (Fig. 12). When VLP-coated plates were preincubated with an epitope A human MAb, binding of a mouse epitope A MAb was reduced. The epitope A human MAb blocked 50% of the binding of a mouse epitope A MAb at 0.7325 μg/ml for GII.4.1997 and 0.1419 μg/ml for GII.4.2006. Binding of the epitope A human MAb did not affect binding of the mouse MAb GII.4.2002.G5 for either VLP. Likewise, a strain-mismatched epitope A human MAb did not affect binding of either the mouse epitope A or GII.4.2002.G5 antibody for either VLP. Conversely, preincubation of the VLP with NVB 71.4 did not affect binding of the mouse epitope A MAbs but decreased binding of GII.4.2002.G5. NVB 71.4 human MAb blocked 50% of the binding of mouse GII.4.2002.G5 at 0.0982 μg/ml for GII.4.1997 and 0.1913 μg/ml for GII.4.2006. Combined, these data indicate that VLPs bound by NVB 71.4 retain conformation and spatial flexibility for interaction with molecules that bind to the particle surface, suggesting neither particle disassembly nor steric hindrance is likely to explain NVB 71.4 blockade activity.

DISCUSSION

The extensive burden of NoV disease on both pre- and postindustrialized nations warrants World Health Organization support for development of a NoV vaccine. A new GII.4 strain has emerged every 3 to 4 years since 2002, and the newly emergent strain, with altered blockade epitopes, has quickly spread globally thorough immunologically naive populations, highlighting a significant hurdle to successful NoV vaccination regimens. Extensive work has documented the antigenic changes in epitope A that correlate with GII.4 strain emergence (35, 36, 42, 46), providing a possible surveillance target for NoV monitoring. Epitope D remained fairly static until GII.4.2012 Sydney mutations resulted in a loss of blockade activity by human MAb NVB 97 (46). While the biological relevance of both epitopes A and D has been confirmed with human MAbs, the natural variation within these epitopes makes them difficult targets for antigen-based vaccine design.

In comparison, blockade epitopes conserved among multiple epidemiologically important strains of virus, including herd immunity escape mutants, provide potential targets for broadly protective vaccines, and the antibodies that recognize these epitopes provide potential diagnostic and therapeutic reagents (50). Recently, Hansman et al. (62) reported a linear GII NoV conserved antibody epitope that is exposed transiently by proposed changes in particle conformation. This antibody was not tested for blockade capacity and is unlikely to recognize the GII.4 conformation-dependent conserved blockade epitope. The conserved GII.4 blockade epitopes recognized by human MAb NVB 71.4 and mouse MAb GII.4.2002.G5 likely overlap but are not identical, as NVB 71.4 can compete with GII.4.2002.G5 binding but NVB 71.4 has a higher blockade capacity and a different preferential blockade pattern across a panel of time-ordered GII.4 VLPs.

The concept of viral capsids as dynamic structures that can assume different conformations is a well-established assumption

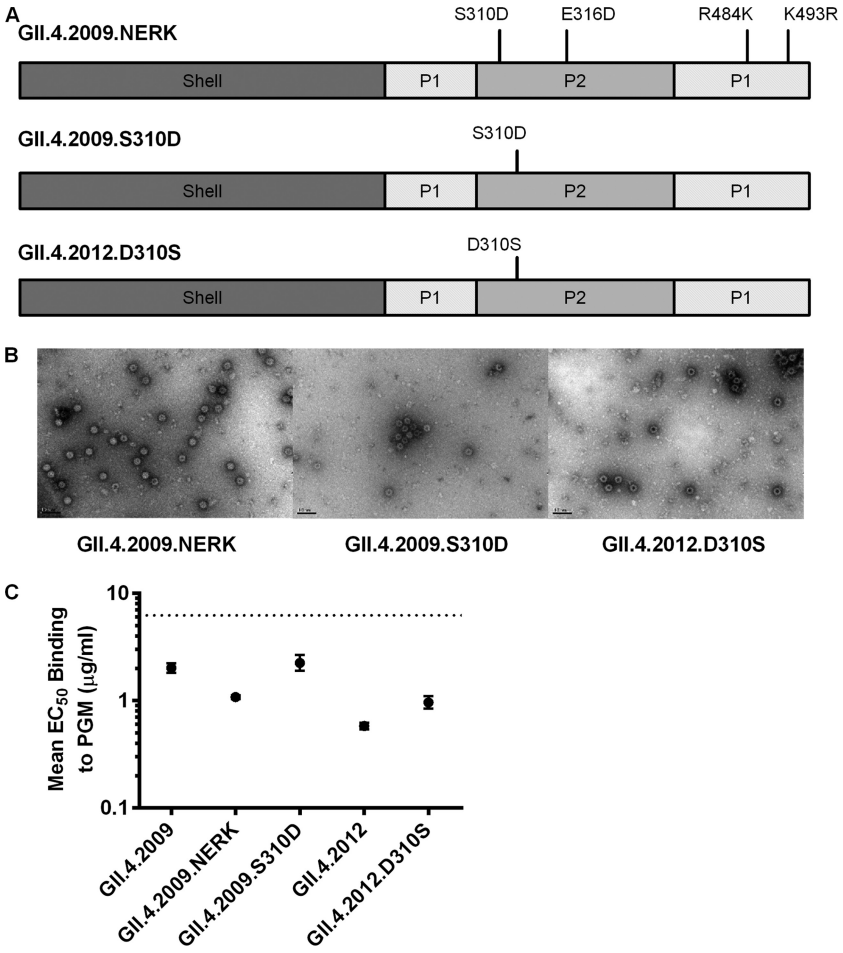

FIG 9 Characterization of VLPs with substitutions in residue 310 and NERK. (A) Schematic of constructs. (B and C) Particle integrity was verified by transmission electron microscope visualization (B) and carbohydrate ligand (PGM) binding of VLPs (C). The dotted line marks the upper limit of detection in panel C. The error bars represent 95% confidence intervals. Scale bars, 100 nm.

in virology. Here, we map specific residues that mediate possible conformation subsets, which may be important for manufacturing NoV VLP-based vaccines. Despite identifying residue changes that affect the blockade capacities of NVB 71.4 and GII.4.2002.G5, we have not identified the epitope(s) that actually binds these MAbs. For both MAbs, K_d and EC_{50} values were less than 2-fold different between GII.4.2006 and GII.4.2006.ERK, and while ERK substitutions decrease the blockade potency of the antibodies, they do not eliminate the impact of elevated temperature on blockade. Further, blockade of GII.4.2006 and GII.4.2006.ERK with NVB 71.4 Fab fragments reduces the effect of ERK substitutions while maintaining the effect of temperature on blockade. These data clearly indicate that the effect of the ERK motif on MAb blockade is not the result of loss of antibody binding to the epitope but instead suggest that ERK regulates antibody blockade capacity by regulating functional access to the epitope itself. Previous work with polio virus (60) and West Nile virus (59) has shown that temperature affects particle dynamics or "breathing" and subsequently antibody access to nonsurface epitopes. In both cases, at 37°C, viruses are dynamic structures reversibly exposing internal antibody epitopes that are concealed at 25°C. Elegant studies with flaviviruses have carefully dissected the impacts of residue changes, time, and temperature on monoclonal antibody neutralization (59, 63). Similar to observations reported here, for many antibodies, the effect was less than 1 log unit of neutralization titer. Given the limited impact of ERK changes on the temperature dependence of blockade, the ERK domain may lie near the antibody epitopes and influence blockade through an allosteric effect by altering the environment surrounding the epitopes, or it may conformation shield the epitope from the antibody. Why GII.4 NoVs occlude the conserved blockade epitope at room temperature but not 37°C is unknown, but it suggests that the epitope may be essential for infection and thus need to be exposed in the host (37°C) but is also susceptible to degradation and thus needs to be protected in the external environment, where infection is not a viable option. In the absence of a feasible infection model and a GII.4 molecular clone, it is not possible to evaluate the relationship between different particle conformations (epitope accessible versus not accessible) and infectious virus. Blockade of residue 310 mutant VLPs indicates that 310 is a conformational regulator of access to the conserved blockade epitopes in multiple GII.4 backgrounds. Comparing blockade of GII.4.2009 (S310), GII.4.2006 (N310), GII.4.2012 (D310), GII.4.2009.S310D, and GII.4.2012.D310S VLPs, all in the context of the conserved ERK motif, supports a role for residue 310 in the accessibility of the conserved blockade epitope. Our data suggest that an aspartic acid

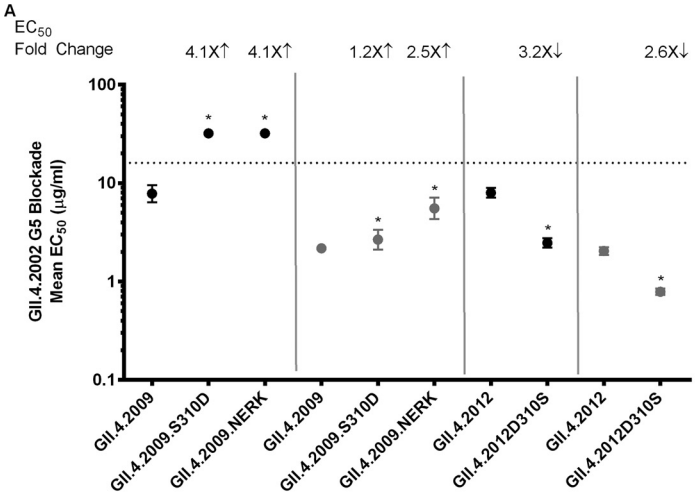

B

mab	NVB 71.4 Fab		NVB 71.4 IgG		GII.4.2002.G5	
VLP	Potency	Temperature Sensitivity	Potency	Temperature Sensitivity	Potency	Temperature Sensitivity
GII.4.2009.S310D	2.8	8.0	2.0	10.5	4.1	12.0
GII.4.2012.D310S	1.0	5.4	2.7	4.6	3.2	3.1
GII.4.2009.NERK	1.0	2.4	1.2	4.6	4.1	5.8

FIG 10 Residue 310 inversely modulates blockade potency and temperature sensitivity of the conserved GII.4 epitope. GII.4.2002.G5 (A and B) and NVB 71.4 Fab fragments and NVB 71.4 IgG (B) were assayed for the ability to block the interaction of VLPs with carbohydrate ligand at room temperature (solid circles) and at 37°C (grey circles). Sigmoidal curves were fitted to the mean percent control binding (the percentage of VLPs bound to ligand in the presence of antibody pretreatment compared to the number of VLPs bound in the absence of antibody pretreatment), and the mean EC_{50} titer for blockade was calculated. (A and B) The fold change in potency (EC_{50} titer) was defined as the ratio between mutant VLPs and wild-type VLPs at room temperature. (B) The fold change (arrow denotes increase or decrease) in temperature sensitivity was defined as the change in the ratio between the mean EC_{50} at 37°C and that at room temperature for the mutant VLPs compared to the ratio at both temperatures for the wild-type VLPs. *, mean EC_{50} blockade titer for mutant VLPs significantly different from the mean EC_{50} blockade titer for wild-type VLPs at the same temperature. The error bars represent 95% confidence intervals. Light shading, fold increase; dark shading, fold decrease.

at position 310 limits access to the epitope more than a serine. Our structural analyses did not have sufficient resolution to explain the impacts of different amino acids at position 310. Importantly, residue 310 exchanges did not completely recapitulate the wild-type VLP blockade temperature phenotype, suggesting that either additional residues likely impact antibody access to the conserved GII.4 blockade epitope or that residues within the actual epitope vary somewhat between the two strains. Detailed crystallography studies of antibody-bound particles are needed to answer these fundamental questions.

Although the mechanisms of antibody blockade of VLP-carbohydrate binding are not known, the correlation between the antibody blockade titer and protection from infection and illness has been documented (15, 41). The location of the ERK motif on the underside of the P domain suggests that NVB 71.4 and GII.4.2002.G5 do not block VLP-ligand interaction by providing a physical barrier between the VLP and the carbohydrate ligand, as is proposed for antibodies to the surface-exposed epitopes A, D, and E (Fig. 13) (35, 36, 47). This hypothesis is supported by observations that NVB 71.4 binding to VLPs does not disrupt binding of antibody to surface epitope A and that antibody Fab fragments retain blockade activity for GII.4 VLPs. Blockade of VLP-ligand binding is also not a function of antibody-mediated particle disassembly or the result of the antibody binding to already disassembled particles, as MAb staining of NVB 71.4-labeled VLPs identified only intact particles. Instead, we hypothesize that NVB 71.4 and GII.4.2002.G5 likely block VLP-ligand interaction by altering the VLP conformation, i.e., by positioning the VLPs in an epitope-accessible conformation (with full antibody access to the conserved blockade epitope) that is unfavorable for ligand binding (Fig. 14). Whether ligand binding is dependent upon the VLP being in an epitope-restricted conformation (with limited antibody access to the conserved blockade epitope) or the actual transition between epitope accessible and epitope restricted is key for ligand binding has yet to be determined. These results mimic well-defined neutralization processes for antibodies that recognize conformation-shielded, conserved neutralization epitopes in a diverse group of RNA viruses, including the E protein DI domain of West Nile virus (59, 64), the gp120 component of the Env protein of HIV (65, 66), and the hemagglutinin stem of influenza virus type A (66, 67). Interestingly, each of these epitopes has residues in structural motifs that are either directly or indirectly involved in viral entry and fusion processes, further suggesting that the antibodies described here may neutralize GII.4 NoV strains by blocking the virus entry/uncoating mechanisms, although this is speculative.

Further study of GII.4.2009 VLPs produced in an insect cell expression system at lower temperature provides support for the relationship between viral conformation and antibody blockade. Blockade of Bac-GII.4.2009 by NVB 71.4 and GII.4.2005.G5 is potent and not temperature dependent, suggesting that the native conformation of GII.4.2009 in this system highly favors the

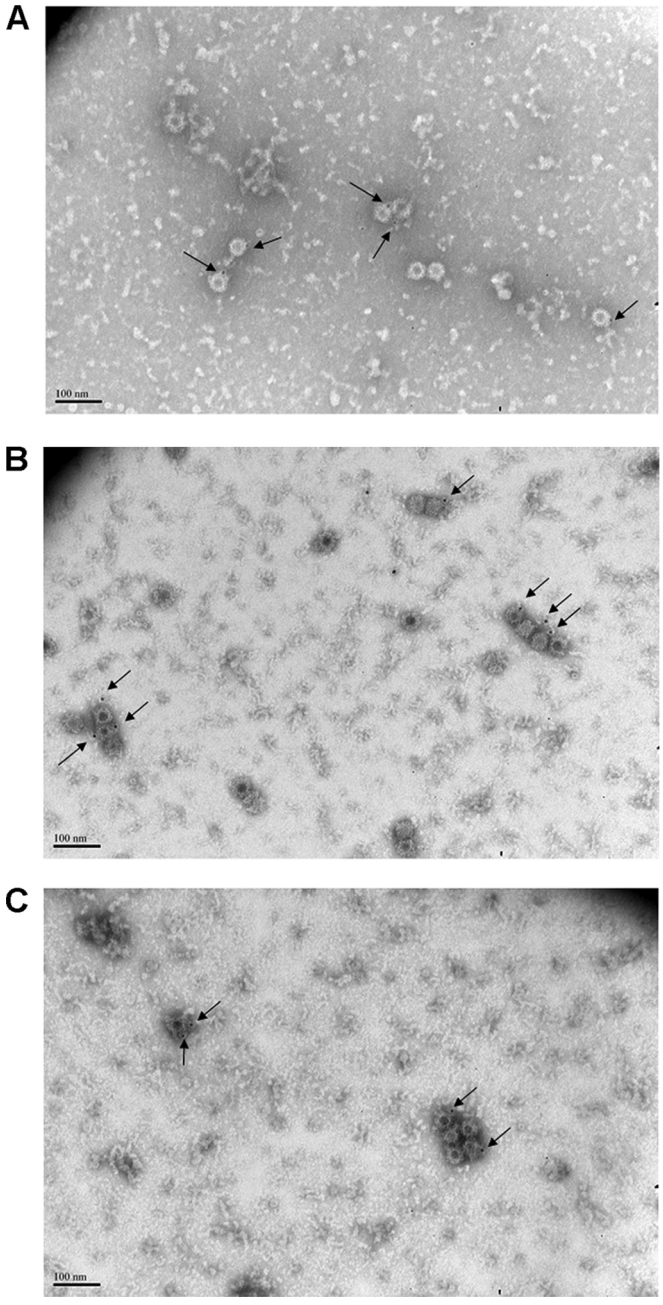

FIG 11 Antibody-bound VLPs retain structural integrity. GII.4.2009 (A and C) and GII.4.2009.NERK (B) VLPs were immunostained with NVB 71.4 (A and B) or epitope A (C) human MAbs and visualized by negative-stain transmission electron microscopy. The arrows indicate immunogold-labeled VLPs.

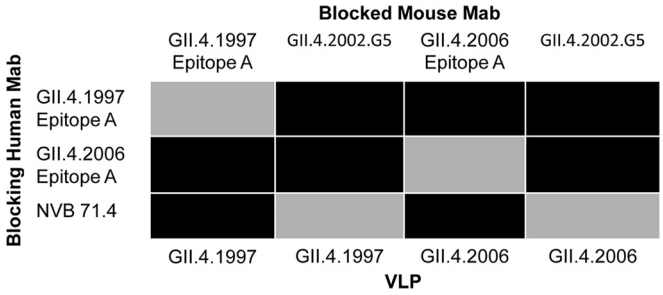

FIG 12 Binding of NVB 71.4 does not disrupt surface epitope A topology. Human MAbs to surface epitope A or NVB 71.4 were evaluated for the ability to block binding of mouse MAbs to epitope A or the conserved blockade epitope in GII.4.1997 (A) and GII.4.2006 (B) using a BOB assay. Sigmoidal curves were fitted to the mean percent control binding (the percentage of mouse MAb bound to VLPs in the presence of human MAb pretreatment compared to the amount of mouse MAb bound in the absence of human MAb pretreatment), and the mean EC_{50} titer for blockade of binding was calculated. Black shading, $EC_{50} > 8$ μg/ml; grey shading, $EC_{50} < 1$ μg/ml.

"epitope-accessible" form. Conversely, GII.4.2009 VLPs made in a mammalian expression system at 37°C require more antibody for blockade and the blockade is temperature sensitive, indicating that the particle assembly conditions can affect particle structure, epitope access, and, subsequently, blockade potency for NVB 71.4 and GII.4.2002.G5. Even though the primary nucleotide sequences of the exogenous genes are identical in the insect cell vector and the mammalian cell vector, multiple factors could explain the difference between the two GII.4.2009 VLPs, including posttranslational protein processing, temperature of particle assembly, and particle purification and storage conditions, all factors that could impact particle structure. Previous detailed studies of Norwalk virus VLPs produced in insect cells indicated that the VLPs undergo structural changes at high temperature (>50°C) and pH (>8) but are stable at the pH and temperatures of the blockade assay (68). How these studies with Norwalk virus VLPs relate to the GII.4 VLPs studied here is unknown, as others have shown that Norwalk and GII.4 VLPs have different pH-dependent ligand binding characteristics (54). In agreement with the results of Tian et al. (54), pH did not affect ligand binding of the GII.4 VLPs we tested (data not shown). Although temperature affects both the kinetics and affinities of molecular interactions, temperature alone is unlikely to explain the difference, as VLPs made by infecting mammalian cells at 30°C with GII.4.2009 VRPs resulted in VLPs with the same antibody blockade potency and temperature dependence as VLPs made at 37°C from the same VRP. These data suggest that factors outside the primary nucleotide sequence, including the host cell, may affect particle formation in subtle ways and antibody neutralization potential in significant ways. If the observed differences between the two GII.4.2009 VLPs studied here is the direct result of VLP production in the baculovirus vector system, this is key information for manufacturing the baculovirus-produced VLP NoV vaccine currently in phase I study, as computational studies on human papillomavirus suggest that limiting structural fluctuations should produce better vaccine immunogens (69). While the Bac-GII.4.2009 VLPs clearly allow better antibody access to the epitopes for NVB 71.4 and GII.4.2002.G5 than VLPs made using VRPs in the mammalian system, it seems likely that other subsurface blockade epitopes will be less accessible on the Bac-GII.4.2009 VLP. Detailed crystallography studies of antibody-bound particles are needed to answer these fundamental questions about VLP structure and how it impacts cross-strain blockade antibody responses. However, all of the crystallography studies on NoV VLPs have been done on baculovirus or other nonmammalian cell culture-derived proteins. Given the observations presented here, the field should consider evaluating VLPs produced in additional mammalian-based systems.

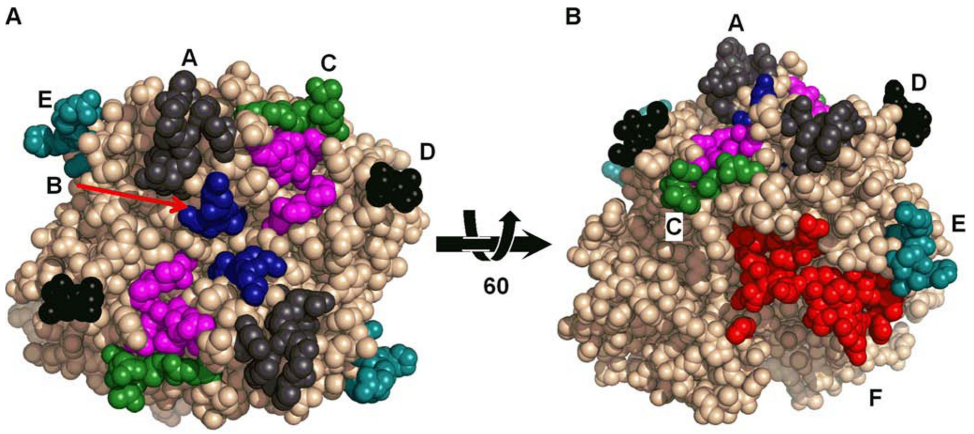

FIG 13 Mapped epitopes of GII.4 noroviruses. (A) The previously described evolving antibody blockade epitopes A to E are on the surface next to the carbohydrate binding sites (pink). (B) The NERK motif (red) is distal to the carbohydrate binding sites (pink).

Antibodies to conserved GII.4 NoV blockade epitopes have important therapeutic and vaccine potential. Human MAb NVB 71.4 could be administered prophylactically for acute or chronic illness (70). More importantly, the antibody could be used as a probe for antigen panning to identify the conserved blockade epitope. The epitope could possibly then subsequently be genetically engineered to have better access within an immunizing VLP. The supposition that locking the VLP in an epitope-accessible conformation prevents ligand binding suggests that a drug that could similarly lock the viral conformation could be an effective broad-based NoV treatment, as has been described for rhinovirus treatment with WIN compounds (71). Further, these observations open lines of inquiry into the mechanisms of human NoV entry and uncoating, presenting fundamental biological questions that are currently unanswerable for these noncultivatable pathogens.

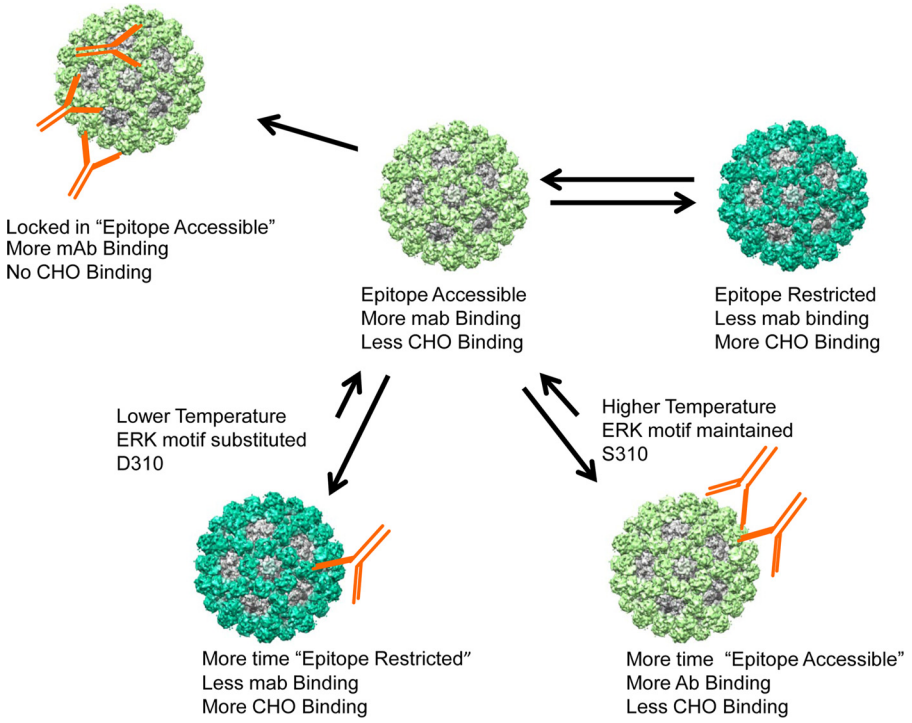

FIG 14 Proposed model for regulation of antibody access to the conserved GII.4 blockade epitope(s) by the NERK motif and VLP structural conformation. GII.4 NoV VLPs produced in mammalian cells can exist in multiple conformations. Two possibilities are represented by the light- and dark-green VLP shading. Antibody access to the conserved GII.4 blockade epitope is different in the two states. Antibody "locking" of the particle into an epitope-accessible conformation prevents ligand binding and allows more antibody blockade activity. Further, antibody access to the conserved GII.4 blockade epitope can be regulated by the temperature and residues outside the antibody binding site. Elevated temperature or a serine at residue 310 favors antibody access to the epitope and subsequently more blockade activity, whereas lower temperature or an aspartic acid at position 310 restricts antibody access to the epitope, resulting in less blockade activity.

ACKNOWLEDGMENTS

We thank Victoria Madden and C. Robert Bagnell, Jr., of the Microscopy Services Laboratory, Department of Pathology and Laboratory Medicine, University of North Carolina—Chapel Hill, for expert technical support and David Jarrossay of the Institute for Research in Biomedicine, Bellinzona, Switzerland, for cell sorting.

This work was supported by a grant from the National Institutes of Health, National Institute of Allergy and Infectious Diseases (AI056351). The funders had no role in study design, data collection and analysis, decision to publish, or preparation of the manuscript.

REFERENCES

1. **CDC.** 2011. Updated norovirus outbreak management and disease prevention guidelines. MMWR Recommend. Rep. **60**(RR-3):1–18.
2. **Hoffmann S, Batz MB, Morris JG, Jr.** 2012. Annual cost of illness and quality-adjusted life year losses in the United States due to 14 foodborne pathogens. J. Food Prot. **75:**1292–1302. http://dx.doi.org/10.4315/0362-028X.JFP-11-417.
3. **Patel MM, Widdowson MA, Glass RI, Akazawa K, Vinje J, Parashar UD.** 2008. Systematic literature review of role of noroviruses in sporadic gastroenteritis. Emerg. Infect. Dis. **14:**1224–1231. http://dx.doi.org/10.3201/eid1408.071114.
4. **Trivedi TK, Desai R, Hall AJ, Patel M, Parashar UD, Lopman BA.** 2013. Clinical characteristics of norovirus-associated deaths: a systematic literature review. Am. J. Infect. Control **41:**654–657. http://dx.doi.org/10.1016/j.ajic.2012.08.002.
5. **Bok K, Green KY.** 2012. Norovirus gastroenteritis in immunocompromised patients. N. Engl. J. Med. **367:**2126–2132. http://dx.doi.org/10.1056/NEJMra1207742.
6. **Trivedi TK, DeSalvo T, Lee L, Palumbo A, Moll M, Curns A, Hall AJ, Patel M, Parashar UD, Lopman BA.** 2012. Hospitalizations and mortality associated with norovirus outbreaks in nursing homes, 2009–2010. JAMA **308:**1668–1675. http://dx.doi.org/10.1001/jama.2012.14023.
7. **Hutson AM, Atmar RL, Estes MK.** 2004. Norovirus disease: changing epidemiology and host susceptibility factors. Trends Microbiol. **12:**279–287. http://dx.doi.org/10.1016/j.tim.2004.04.005.
8. **Estes MK, Prasad BV, Atmar RL.** 2006. Noroviruses everywhere: has something changed? Curr. Opin. Infect. Dis. **19:**467–474. http://dx.doi.org/10.1097/01.qco.0000244053.69253.3d.
9. **Koopmans M, Vinjé J, de Wit M, Leenen I, van der Poel W, van Duynhoven Y.** 2000. Molecular epidemiology of human enteric caliciviruses in The Netherlands. J. Infect. Dis. **181**(Suppl 2):S262–S269. http://dx.doi.org/10.1086/315573.
10. **CDC.** 2007. Norovirus activity—United States, 2006–2007. MMWR Morb. Mortal. Wkly. Rep. **56:**842–846.
11. **Okada M, Tanaka T, Oseto M, Takeda N, Shinozaki K.** 2006. Genetic analysis of noroviruses associated with fatalities in healthcare facilities. Arch. Virol. **151:**1635–1641. http://dx.doi.org/10.1007/s00705-006-0739-6.
12. **Harris JP, Edmunds WJ, Pebody R, Brown DW, Lopman BA.** 2008. Deaths from norovirus among the elderly, England and Wales. Emerg. Infect. Dis. **14:**1546–1552. http://dx.doi.org/10.3201/eid1410.080188.
13. **Schorn R, Hohne M, Meerbach A, Bossart W, Wuthrich RP, Schreier E, Muller NJ, Fehr T.** 2010. Chronic norovirus infection after kidney transplantation: molecular evidence for immune-driven viral evolution. Clin. Infect. Dis. **51:**307–314. http://dx.doi.org/10.1086/653939.
14. **Hall AJ, Eisenbart VG, Etingue AL, Gould LH, Lopman BA, Parashar UD.** 2012. Epidemiology of foodborne norovirus outbreaks, United States, 2001–2008. Emerg. Infect. Dis. **18:**1566–1573. http://dx.doi.org/10.3201/eid1810.120833.
15. **Atmar RL, Bernstein DI, Harro CD, Al-Ibrahim MS, Chen WH, Ferreira J, Estes MK, Graham DY, Opekun AR, Richardson C, Mendelman PM.** 2011. Norovirus vaccine against experimental human Norwalk Virus illness. N. Engl. J. Med. **365:**2178–2187. http://dx.doi.org/10.1056/NEJMoa1101245.
16. **Richardson C, Bargatze RF, Goodwin R, Mendelman PM.** 2013. Norovirus virus-like particle vaccines for the prevention of acute gastroenteritis. Expert Rev. Vaccines **12:**155–167. http://dx.doi.org/10.1586/erv.12.145.
17. **Noel JS, Fankhauser RL, Ando T, Monroe SS, Glass RI.** 1999. Identification of a distinct common strain of "Norwalk-like viruses" having a global distribution. J. Infect. Dis. **179:**1334–1344. http://dx.doi.org/10.1086/314783.
18. **Vinje J, Altena S, Koopmans M.** 1997. The incidence and genetic variability of small round-structured viruses in outbreaks of gastroenteritis in the Netherlands. J. Infect. Dis. **176:**1374–1378. http://dx.doi.org/10.1086/517325.
19. **Widdowson MA, Cramer EH, Hadley L, Bresee JS, Beard RS, Bulens SN, Charles M, Chege W, Isakbaeva E, Wright JG, Mintz E, Forney D, Massey J, Glass RI, Monroe SS.** 2004. Outbreaks of acute gastroenteritis on cruise ships and on land: identification of a predominant circulating strain of norovirus—United States, 2002. J. Infect. Dis. **190:**27–36. http://dx.doi.org/10.1086/420888.
20. **Bull RA, Tu ET, McIver CJ, Rawlinson WD, White PA.** 2006. Emergence of a new norovirus genotype II.4 variant associated with global outbreaks of gastroenteritis. J. Clin. Microbiol. **44:**327–333. http://dx.doi.org/10.1128/JCM.44.2.327-333.2006.
21. **Kroneman A, Vennema H, Harris J, Reuter G, von Bonsdorff CH, Hedlund KO, Vainio K, Jackson V, Pothier P, Koch J, Schreier E, Bottiger BE, Koopmans M.** 2006. Increase in norovirus activity reported in Europe. Euro Surveill. **11:**E061214.1.
22. **Phan TG, Kuroiwa T, Kaneshi K, Ueda Y, Nakaya S, Nishimura S, Yamamoto A, Sugita K, Nishimura T, Yagyu F, Okitsu S, Muller WE, Maneekarn N, Ushijima H.** 2006. Changing distribution of norovirus genotypes and genetic analysis of recombinant GIIb among infants and children with diarrhea in Japan. J. Med. Virol. **78:**971–978. http://dx.doi.org/10.1002/jmv.20649.
23. **Siebenga J, Kroneman A, Vennema H, Duizer E, Koopmans M.** 2008. Food-borne viruses in Europe network report: the norovirus GII.4 2006b (for US named Minerva-like, for Japan Kobe034-like, for UK V6) variant now dominant in early seasonal surveillance. Euro Surveill. **13:**8009.
24. **Vega EBL, Gregoricus N, Williams K, Lee D, Vinjé J.** 2011. Novel surveillance network for norovirus gastroenteritis outbreaks, United States. Emerg. Infect. Dis. **17:**1389–1395. http://dx.doi.org/10.3201/eid1708.101837.
25. **CDC.** 2013. Emergence of new norovirus strain GII.4 Sydney—United States, 2012. MMWR Morb. Mortal. Wkly. Rep. **62:**55.
26. **van Beek J, Ambert-Balay K, Botteldoorn N, Eden JS, Fonager J, Hewitt J, Iritani N, Kroneman A, Vennema H, Vinje J, White PA, Koopmans M.** 2013. Indications for worldwide increased norovirus activity associated with emergence of a new variant of genotype II.4, late 2012. Euro Surveill. **18:**8–9.
27. **Siebenga JJ, Vennema H, Renckens B, de Bruin E, van der Veer B, Siezen RJ, Koopmans M.** 2007. Epochal evolution of GGII.4 norovirus capsid proteins from 1995 to 2006. J. Virol. **81:**9932–9941. http://dx.doi.org/10.1128/JVI.00674-07.
28. **Lindesmith LC, Donaldson EF, Lobue AD, Cannon JL, Zheng DP, Vinje J, Baric RS.** 2008. Mechanisms of GII. 4 norovirus persistence in human populations. PLoS Med. **5:**e31. http://dx.doi.org/10.1371/journal.pmed.0050031.
29. **Zheng DP, Ando T, Fankhauser RL, Beard RS, Glass RI, Monroe SS.** 2006. Norovirus classification and proposed strain nomenclature. Virology **346:**312–323. http://dx.doi.org/10.1016/j.virol.2005.11.015.
30. **Baric RS, Yount B, Lindesmith L, Harrington PR, Greene SR, Tseng FC, Davis N, Johnston RE, Klapper DG, Moe CL.** 2002. Expression and self-assembly of Norwalk virus capsid protein from Venezuelan equine encephalitis virus replicons. J. Virol. **76:**3023–3030. http://dx.doi.org/10.1128/JVI.76.6.3023-3030.2002.
31. **Prasad BV, Hardy ME, Dokland T, Bella J, Rossmann MG, Estes MK.** 1999. X-ray crystallographic structure of the Norwalk virus capsid. Science **286:**287–290. http://dx.doi.org/10.1126/science.286.5438.287.
32. **Chen R, Neill JD, Estes MK, Prasad BV.** 2006. X-ray structure of a native calicivirus: structural insights into antigenic diversity and host specificity. Proc. Natl. Acad. Sci. U. S. A. **103:**8048–8053. http://dx.doi.org/10.1073/pnas.0600421103.
33. **Lochridge VP, Jutila KL, Graff JW, Hardy ME.** 2005. Epitopes in the P2 domain of norovirus VP1 recognized by monoclonal antibodies that block cell interactions. J. Gen. Virol. **86:**2799–2806. http://dx.doi.org/10.1099/vir.0.81134-0.
34. **Cao S, Lou Z, Tan M, Chen Y, Liu Y, Zhang Z, Zhang XC, Jiang X, Li X, Rao Z.** 2007. Structural basis for the recognition of blood group trisaccharides by norovirus. J. Virol. **81:**5949–5957. http://dx.doi.org/10.1128/JVI.00219-07.
35. **Debbink K, Donaldson EF, Lindesmith LC, Baric RS.** 2012. Genetic

mapping of a highly variable norovirus GII.4 blockade epitope: potential role in escape from human herd immunity. J. Virol. **86:**1214–1226. http://dx.doi.org/10.1128/JVI.06189-11.
36. **Lindesmith LC, Debbink K, Swanstrom J, Vinje J, Costantini V, Baric RS, Donaldson EF.** 2012. Monoclonal antibody-based antigenic mapping of norovirus GII.4-2002. J. Virol. **86:**873–883. http://dx.doi.org/10.1128/JVI.06200-11.
37. **Cannon JL, Lindesmith LC, Donaldson EF, Saxe L, Baric RS, Vinje J.** 2009. Herd immunity to GII.4 noroviruses is supported by outbreak patient sera. J. Virol. **83:**5363–5374. http://dx.doi.org/10.1128/JVI.02518-08.
38. **Harrington PR, Lindesmith L, Yount B, Moe CL, Baric RS.** 2002. Binding of Norwalk virus-like particles to ABH histo-blood group antigens is blocked by antisera from infected human volunteers or experimentally vaccinated mice. J. Virol. **76:**12335–12343. http://dx.doi.org/10.1128/JVI.76.23.12335-12343.2002.
39. **Lindesmith LC, Donaldson E, Leon J, Moe CL, Frelinger JA, Johnston RE, Weber DJ, Baric RS.** 2010. Heterotypic humoral and cellular immune responses following Norwalk virus infection. J. Virol. **84:**1800–1815. http://dx.doi.org/10.1128/JVI.02179-09.
40. **Bok K, Parra GI, Mitra T, Abente E, Shaver CK, Boon D, Engle R, Yu C, Kapikian AZ, Sosnovtsev SV, Purcell RH, Green KY.** 2011. Chimpanzees as an animal model for human norovirus infection and vaccine development. Proc. Natl. Acad. Sci. U. S. A. **108:**325–330. http://dx.doi.org/10.1073/pnas.1014577107.
41. **Reeck A, Kavanagh O, Estes MK, Opekun AR, Gilger MA, Graham DY, Atmar RL.** 2010. Serological correlate of protection against norovirus-induced gastroenteritis. J. Infect. Dis. **202:**1212–1218. http://dx.doi.org/10.1086/656364.
42. **Lindesmith LC, Costantini V, Swanstrom J, Debbink K, Donaldson EF, Vinje J, Baric RS.** 2013. Emergence of a norovirus GII.4 strain correlates with changes in evolving blockade epitopes. J. Virol. **87:**2803–2813. http://dx.doi.org/10.1128/JVI.03106-12.
43. **Eden JS, Tanaka MM, Boni MF, Rawlinson WD, White PA.** 2013. Recombination within the pandemic norovirus GII.4 lineage. J. Virol. **87:**6270–6282. http://dx.doi.org/10.1128/JVI.03464-12.
44. **Bull RA, Eden JS, Rawlinson WD, White PA.** 2010. Rapid evolution of pandemic noroviruses of the GII.4 lineage. PLoS Pathog. **6:**e1000831. http://dx.doi.org/10.1371/journal.ppat.1000831.
45. **Siebenga JJ, Lemey P, Kosakovsky S, Pond L, Rambaut A, Vennema H, Koopmans M.** 2010. Phylodynamic reconstruction reveals norovirus GII.4 epidemic expansions and their molecular determinants. PLoS Pathog. **6:**e1000884. http://dx.doi.org/10.1371/journal.ppat.1000884.
46. **Debbink K, Lindesmith LC, Donaldson EF, Costantini V, Beltramello M, Corti D, Swanstrom J, Lanzavecchia A, Vinje J, Baric RS.** 2013. Emergence of new pandemic GII.4 Sydney norovirus strain correlates with escape from herd immunity. J. Infect. Dis. **208:**1877–1887. http://dx.doi.org/10.1093/infdis/jit370.
47. **Lindesmith LC, Beltramello M, Donaldson EF, Corti D, Swanstrom J, Debbink K, Lanzavecchia A, Baric RS.** 2012. Immunogenetic mechanisms driving norovirus GII.4 antigenic variation. PLoS Pathog. **8:**e1002705. http://dx.doi.org/10.1371/journal.ppat.1002705.
48. **Allen DJ, Gray JJ, Gallimore CI, Xerry J, Iturriza-Gomara M.** 2008. Analysis of amino acid variation in the P2 domain of the GII-4 norovirus VP1 protein reveals putative variant-specific epitopes. PLoS One **3:**e1485. http://dx.doi.org/10.1371/journal.pone.0001485.
49. **Donaldson EF, Lindesmith LC, Lobue AD, Baric RS.** 2008. Norovirus pathogenesis: mechanisms of persistence and immune evasion in human populations. Immunol. Rev. **225:**190–211. http://dx.doi.org/10.1111/j.1600-065X.2008.00680.x.
50. **Belliot G, Noel JS, Li JF, Seto Y, Humphrey CD, Ando T, Glass RI, Monroe SS.** 2001. Characterization of capsid genes, expressed in the baculovirus system, of three new genetically distinct strains of "Norwalk-like viruses". J. Clin. Microbiol. **39:**4288–4295. http://dx.doi.org/10.1128/JCM.39.12.4288-4295.2001.
51. **Lindesmith LC, Donaldson EF, Baric RS.** 2011. Norovirus GII.4 strain antigenic variation. J. Virol. **85:**231–242. http://dx.doi.org/10.1128/JVI.01364-10.
52. **Larkin MA, Blackshields G, Brown NP, Chenna R, McGettigan PA, McWilliam H, Valentin F, Wallace IM, Wilm A, Lopez R, Thompson JD, Gibson TJ, Higgins DG.** 2007. Clustal W and Clustal X version 2.0. Bioinformatics **23:**2947–2948. http://dx.doi.org/10.1093/bioinformatics/btm404.
53. **Shanker S, Choi JM, Sankaran B, Atmar RL, Estes MK, Prasad BV.** 2011. Structural analysis of HBGA binding specificity in a norovirus GII.4 epidemic variant: implications for epochal evolution. J. Virol. **85:**8635–8645. http://dx.doi.org/10.1128/JVI.00848-11.
54. **Tian P, Yang D, Jiang X, Zhong W, Cannon JL, Burkhardt W, III, Woods JW, Hartman G, Lindesmith L, Baric RS, Mandrell R.** 2010. Specificity and kinetics of norovirus binding to magnetic bead-conjugated histo-blood group antigens. J. Appl. Microbiol. **109:**1753–1762. http://dx.doi.org/10.1111/j.1365-2672.2010.04812.x.
55. **Swanstrom J, Lindesmith LC, Donaldson EF, Yount B, Baric RS.** 2014. Characterization of blockade antibody responses in GII.2.1976 Snow Mountain virus-infected subjects. J. Virol. **88:**829–837. http://dx.doi.org/10.1128/JVI.02793-13.
56. **Lee PD, Mukherjee S, Edeling MA, Dowd KA, Austin SK, Manhart CJ, Diamond MS, Fremont DH, Pierson TC.** 2013. The Fc region of an antibody impacts the neutralization of West Nile viruses in different maturation states. J. Virol. **87:**13729–13740. http://dx.doi.org/10.1128/JVI.02340-13.
57. **Corti D, Langedijk JP, Hinz A, Seaman MS, Vanzetta F, Fernandez-Rodriguez BM, Silacci C, Pinna D, Jarrossay D, Balla-Jhagjhoorsingh S, Willems B, Zekveld MJ, Dreja H, O'Sullivan E, Pade C, Orkin C, Jeffs SA, Montefiori DC, Davis D, Weissenhorn W, McKnight A, Heeney JL, Sallusto F, Sattentau QJ, Weiss RA, Lanzavecchia A.** 2010. Analysis of memory B cell responses and isolation of novel monoclonal antibodies with neutralizing breadth from HIV-1-infected individuals. PLoS One **5:**e8805. http://dx.doi.org/10.1371/journal.pone.0008805.
58. **Sabin C, Corti D, Buzon V, Seaman MS, Lutje Hulsik D, Hinz A, Vanzetta F, Agatic G, Silacci C, Mainetti L, Scarlatti G, Sallusto F, Weiss R, Lanzavecchia A, Weissenhorn W.** 2010. Crystal structure and size-dependent neutralization properties of HK20, a human monoclonal antibody binding to the highly conserved heptad repeat 1 of gp41. PLoS Pathog. **6:**e1001195. http://dx.doi.org/10.1371/journal.ppat.1001195.
59. **Dowd KA, Jost CA, Durbin AP, Whitehead SS, Pierson TC.** 2011. A dynamic landscape for antibody binding modulates antibody-mediated neutralization of West Nile virus. PLoS Pathog. **7:**e1002111. http://dx.doi.org/10.1371/journal.ppat.1002111.
60. **Li Q, Yafal AG, Lee YM, Hogle J, Chow M.** 1994. Poliovirus neutralization by antibodies to internal epitopes of VP4 and VP1 results from reversible exposure of these sequences at physiological temperature. J. Virol. **68:**3965–3970.
61. **Nelson S, Jost CA, Xu Q, Ess J, Martin JE, Oliphant T, Whitehead SS, Durbin AP, Graham BS, Diamond MS, Pierson TC.** 2008. Maturation of West Nile virus modulates sensitivity to antibody-mediated neutralization. PLoS Pathog. **4:**e1000060. http://dx.doi.org/10.1371/journal.ppat.1000060.
62. **Hansman GS, Taylor DW, McLellan JS, Smith TJ, Georgiev I, Tame JR, Park SY, Yamazaki M, Gondaira F, Miki M, Katayama K, Murata K, Kwong PD.** 2012. Structural basis for broad detection of genogroup II noroviruses by a monoclonal antibody that binds to a site occluded in the viral particle. J. Virol. **86:**3635–3646. http://dx.doi.org/10.1128/JVI.06868-11.
63. **VanBlargan LA, Mukherjee S, Dowd KA, Durbin AP, Whitehead SS, Pierson TC.** 2013. The type-specific neutralizing antibody response elicited by a dengue vaccine candidate is focused on two amino acids of the envelope protein. PLoS Pathog. **9:**e1003761. http://dx.doi.org/10.1371/journal.ppat.1003761.
64. **Dowd KA, Pierson TC.** 2011. Antibody-mediated neutralization of flaviviruses: a reductionist view. Virology **411:**306–315. http://dx.doi.org/10.1016/j.virol.2010.12.020.
65. **van Gils MJ, Sanders RW.** 2013. Broadly neutralizing antibodies against HIV-1: templates for a vaccine. Virology **435:**46–56. http://dx.doi.org/10.1016/j.virol.2012.10.004.
66. **Corti D, Lanzavecchia A.** 2013. Broadly neutralizing antiviral antibodies. Annu. Rev. Immunol. **31:**705–742. http://dx.doi.org/10.1146/annurev-immunol-032712-095916.
67. **Stanekova Z, Adkins I, Kosova M, Janulikova J, Sebo P, Vareckova E.** 2013. Heterosubtypic protection against influenza A induced by adenylate cyclase toxoids delivering conserved HA2 subunit of hemagglutinin. Antiviral Res. **97:**24–35. http://dx.doi.org/10.1016/j.antiviral.2012.09.008.
68. **Ausar SF, Foubert TR, Hudson MH, Vedvick TS, Middaugh CR.** 2006. Conformational stability and disassembly of Norwalk virus-like particles. Effect of pH and temperature. J. Biol. Chem. **281:**19478–19488.
69. **Singharoy A, Polavarapu A, Joshi H, Baik MH, Ortoleva P.** 2013.

Epitope fluctuations in the human papillomavirus are under dynamic allosteric control: a computational evaluation of a new vaccine design strategy. J. Am. Chem. Soc. **135:**18458–18468. http://dx.doi.org/10.1021/ja407489r.

70. **Chagla Z, Quirt J, Woodward K, Neary J, Rutherford C.** 2013. Chronic norovirus infection in a transplant patient successfully treated with enterally administered immune globulin. J. Clin. Virol. **58:**306–308. http://dx.doi.org/10.1016/j.jcv.2013.06.009.
71. **Reisdorph N, Thomas JJ, Katpally U, Chase E, Harris K, Siuzdak G, Smith TJ.** 2003. Human rhinovirus capsid dynamics is controlled by canyon flexibility. Virology **314:**34–44. http://dx.doi.org/10.1016/S0042-6822(03)00452-5.